DEVELOPMENT OF NOVEL NANOMATERIALS FOR DISPLAY AND CATALYSIS APPLICATIONS

A THESIS
SUBMITTED TO THE DEPARTMENT OF ADVANCED MATERIALS
AND NANOTECHNOLOGY AND THE GRADUATE SCHOOL OF
NATURAL SCIENCES OF ABDULLAH GÜL UNIVERSITY
IN PARTIAL FULFILLMENT OF THE REQUIREMENTS
FOR THE DEGREE OF
MASTER OF SCIENCE

By
Duygu TAHAOĞLU
January 2016

DEVELOPMENT OF NOVEL NANOMATERIALS FOR DISPLAY AND CATALYSIS APPLICATIONS

A THESIS

SUBMITTED TO THE DEPARTMENT OF ADVANCED MATERIALS AND
NANOTECHNOLOGY AND THE GRADUATE SCHOOL OF NATURAL
SCIENCES OF ABDULLAH GÜL UNIVERSITY
IN PARTIAL FULFILLMENT OF THE REQUIREMENTS
FOR THE DEGREE OF
MASTER OF SCIENCE

By
Duygu TAHAOĞLU
January 2016

I certify that I have read this thesis and that in my opinion it is fully adequate, in scope and in quality, as a thesis for the degree of Master of Science.

_____

Assoc. Prof. Dr. Murat ÇITIR

Supervisor

I certify that I have read this thesis and that in my opinion it is fully adequate, in scope and in quality, as a thesis for the degree of Master of Science.

_____

Assoc. Prof. Dr. Hakan USTA

I certify that I have read this thesis and that in my opinion it is fully adequate, in scope and in quality, as a thesis for the degree of Master of Science.

_____

Assoc. Prof. Dr. Halil ŞAHAN

Approved for the Graduate School of Natural Sciences:

_____

Prof. Dr. İrfan Alan

Director of Graduate School of Natural Sciences

ABSTRACT

DEVELOPMENT OF NOVEL NANOMATERIALS FOR DISPLAY AND CATALYSIS APPLICATIONS

Duygu TAHAOĞLU

M.Sc. in Advanced Materials and Nanotechnology
Supervisor: Assoc. Prof. Dr. Murat ÇITIR

January 2016

Nanomaterials established a research presence due to their large variety and unique properties for many areas such as biotechnology, energy, fabrics, construction, food etc. Transparent conductors and catalysis applications are also two other important areas in which nanomaterial studies are carried out. For display applications, metal nanowires, especially silver and copper, draw too much attention as transparent conductors as an alternative to indium tin oxide (ITO), which is the most used material in this market, due to their high conductivity, low cost and availability for flexible device applications which are limitations for ITO. In catalysis applications, using nanomaterials are also important to provide two essential parameters: increasing the efficiency of reactions and lowering the cost.

In this thesis, on the whole, we present the synthesis of silver and copper nanowires by optimizing some parameters for controlling the length and diameter of nanowires. For the surface passivation of nanowires, we offered some coating methods with noble metals such as gold, platinum and palladium. Also we investigated the catalytic activity of copper nanowires on dye wastewater treatment.

In the first part of this study, effects of polyvinylpyrrolidone (PVP) polymer length and PVP:$AgNO_3$ molar ratio on the efficiency of silver nanowire synthesis and nanowire size were investigated for polyol synthesis method. The results showed that reaction yield is highly depended on these parameters. Also, by using different coating methods such as direct addition or biphasic titration, and by using different noble metal precursors, galvanic exchange reactions on silver nanowire surfaces were studied. The results for coating showed that it is possible to replace silver and noble metal atoms through these methods. The next part of the thesis reports the copper nanowire synthesis

by two different methods: hydrothermal and solution based synthesis. The copper nanowires showed different size properties for these two methods. In addition, the same coating processes were also performed for copper nanowires and the results are promising as silver nanowires. In the last part, catalytic performance of copper nanowires was studied on degradation reactions of three different organic dyes. Great differences between catalyzed and uncatalyzed reaction periods were observed for all dyes.

Keywords: Silver Nanowire, Copper Nanowire, Nanocatalysts, Organic Dye Degradation

ÖZET

EKRAN VE KATALİZ UYGULAMALARI İÇİN YENİ NANOMALZEMELERİN GELİŞTİRİLMESİ

Duygu TAHAOĞLU

İleri Malzemeler ve Nanoteknoloji Anabilim Dalı Yüksek Lisans

Tez Yöneticisi: Doç. Dr. Murat ÇITIR

Ocak 2016

Nanomalzemeler çok çeşitli ve eşsiz özellikleri sayesinde biyoteknoloji, enerji, tekstil, yapı, gıda gibi birçok alanda araştırma konusu olarak yer edinmiştir. Saydam iletkenler ve kataliz uygulamaları, nanomalzeme çalışmalarının yürütüldüğü diğer iki önemli uygulama alanıdır. Ekran uygulamalarında, metal nanoteller, özellikle gümüş ve bakır, yüksek iletkenlik, düşük maliyet ve esnek cihazlara uygulanabilirlik gibi özellikleriyle, ekran piyasasında en çok kullanılan malzeme olan indiyum kalay oksit'e alternatif olarak oldukça ilgi çekmektedir. Kataliz uygulamalarında ise, reaksiyon veriminin artırılması ve maliyetlerin düşürülmesi açısından nanomalzeme kullanımı önemli olmaktadır.

Bu tez çalışmasında, genel olarak, uzunluk ve çap kontrolü için bazı parametrelerin optimizasyonu yapılarak gümüş ve bakır nanotellerin sentezine yer verilmiştir. Sentezlenen nanotellerin oksidasyona açık olması nedeniyle, yüzey pasivasyonu için altın, platin ve paladyum gibi asal metallerle kaplama yöntemleri önerilmiştir. Ayrıca boya atık su arıtımında bakır nanotellerin katalizör etkileri incelenmiştir.

Bu çalışmanın ilk bölümünde, polyol sentez yönteminde kullanılan polivinilpirolidon (PVP) polimerinin molekül uzunluğunun ve PVP/AgNO$_3$ mol oranının gümüş nanotel sentezinin verimi ve nanotel boyutlarına etkisi incelendi. Bu parametrelerin reaksiyon verimine etkisinin büyük olduğu sonucu görüldü. Doğrudan ekleme ve iki fazlı kaplama metotları ve farklı asal metal bileşikleri kullanılarak gümüş nanotel yüzeyinde galvanik reaksiyonlar gerçekleştirildi. Kaplama çalışmaları

sonucunda, bu metotlar kullanılarak nanotel yüzey atomlarının bu asal metallerle değiştirilerek nanotellerin kaplanabildiği görüldü.

Tezin ikinci bölümünde bakır nanotellerin hidrotermal ve çözelti bazlı iki farklı yöntemle sentezlenmesine yer verildi. İki ayrı metotla üretilen nanoteller faklı boyut özelliklerine sahiptir. Gümüş nanotellere uygulanan kaplama yöntemleri, bakır nanoteller için de denendi ve ümit verici kaplama sonuçları elde edildi.

Son bölümde bakır nanotellerin üç farklı organik boyanın degradasyonunda katalizör etkileri çalışıldı. Katalizör kullanımı, 3 boya için de degradasyon süresini çok büyük ölçüde azaltmıştır.

Anahtar kelimeler: Gümüş Nanotel, Bakır Nanotel, Nanokatalizör, Organik Boya Degradasyonu

Acknowledgements

First and foremost, I would like to express my sincere thanks to my advisor Assoc. Prof. Dr. Murat Çıtır for his support, guidance and patience throughout my thesis study. I also would like to thank Assoc. Prof. Dr. Hakan Usta for his advices and guidance for understanding and drawing my way.

I am obliged to my lab-mates Şeyma Dadı and Mehmet Özdemir for their support at every critical moments and their kindness throughout my long laboratory studies. Their support gave me the energy that I need to get through these hard times.

I would like to express my deepest gratitude to my dear friends Yeliz Yoldaş and Abdullah Oran, for their moral support and kindness and Oğuzhan Ayyıldız for his positive, elating and supportive energy which helps me to keep going on my studies.

I also can't deny the patience and moral supports of Hatice Taş and Mustafa Erkartal and I owe them a debt of gratitude.

And finally and the most importantly, I would like to thank my family with my all heart; my precious parents Bahattin and Funda, my dear sister Cansu and my beloved husband Osman, for their endless love, patience and infinite supports for every step in my life.

TABLE OF CONTENTS

LIST OF FIGURES

LIST OF TABLES

To My Family…

Chapter 1

Introduction

Nanoscience is the study of materials in nanoscale (1-100 nm) and can be defined as a subtitle of other science fields, such as chemistry, biology, physics, material science, and engineering [1]. Although nanoscale materials are not new, it hasn't been possible to understand them until microscopy techniques were developed. The development of scanning tunneling microscope (STM) by Gerd Binning and Heinrich Rohrer in 1981 opened a gate to the nano world and gained them a Nobel Prize in 1986 [2]. By the virtue of this invention and the following developments in microscopy techniques, researches at atomic levels could be possible and this brought a large number of discoveries in various fields.

At nanoscale, materials show different phenomena based on the quantum effects and expanded surface area. Therefore, the properties such as melting point, fluorescence, electrical conductivity, optical features, magnetic permeability, and chemical reactivity of the materials change in nano size. By this means, scientist could take the advantage of unique physical, chemical, mechanical, and optical properties which appear at nanoscale differently than bulk materials and used them to develop new processes and technologies in various fields such as medicine, material synthesis, catalysis applications, material science, and many other fields [3].

Decrease in size of structural components of some materials such as crystalline solids causes an increase in interphase area inside the material and this alteration affects the mechanical and electrical properties of materials. For instance, the boundaries between the crystalline grains of metals decelerate and hinder the defect propagation when the material is exposed to a stress. If the material has grains in nanoscale size, so the interface area will be quite high which gains the material a great strength. Nanocrystalline nickel can be given as an example of high strength materials. Because

of its nanosized grains and great interface area, it becomes as strong as hardened steel [4].

In nature, biological systems are entirely based on nanomaterials and nanoprocesses. For instance, hemoglobin molecule in our blood which carries oxygen to our cells is only 5.5 nm and an average DNA is 2 nm in length. To interfere to the biological systems effectively is possible with nanotechnology. By using nanotechnology, more precise and effective treatments with rarer side effects can be applied. For example, gold nanoparticles interact with light differently at nanoscale due to the restricted electron motion. That's why gold nanoparticles look red-purple instead of yellow as in bulk form. Furthermore, gold nanoparticles can selectively accumulate in tumor regions as it's shown in Figure 1.1a. Due to these unique properties of gold nanoparticles, they can be used to find the exact location and to image tumor cells, so tumors can be destroyed by using a targeted laser without damaging healthy cells [3]. In Figure 1.1b, gold nanoparticle use for the cancer detection by modifying the surface with tumor specific antigens was illustrated.
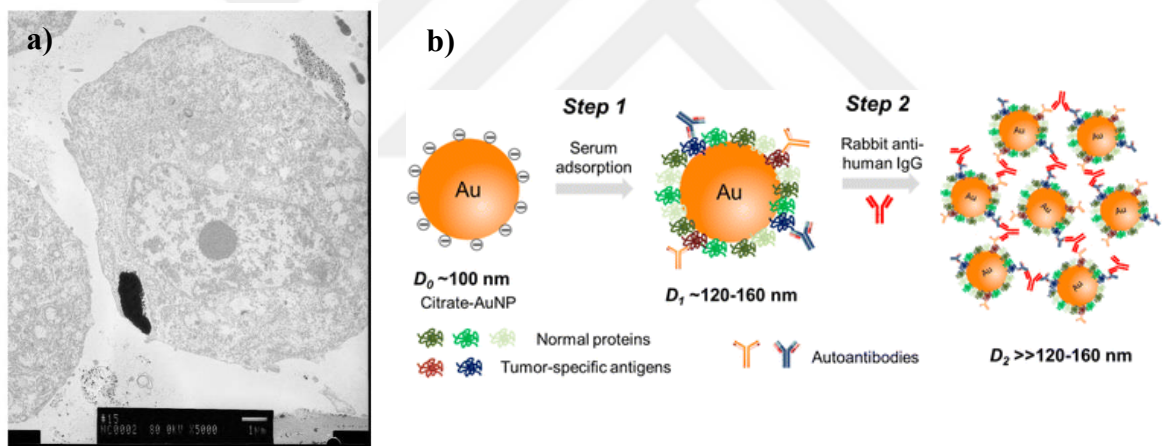
Figure 1.1 a) A breast cancer cell with nanoparticles endocytosed into it [5] **b)** Illustration of a two-step NanoDLSay to analyze the relative amount of human IgG adsorbed to citrate-capped AuNPs for early stage prostate cancer detection [6].

When a material is crumbled into small pieces, surface of the material increases. If the material is split into nano pieces, then the increase of surface area will be tremendous as it's seen in Figure 1.2. Nanomaterials have greater surface area compared to the same amount of bulk materials and higher surface area means higher interaction between the material and its surroundings. As a result, reactivity of the material increases. In catalysis applications, surface area has a great importance for the efficiency of reactions. Nanoscale catalysts technologies have also great and positive effects on economic aspects.
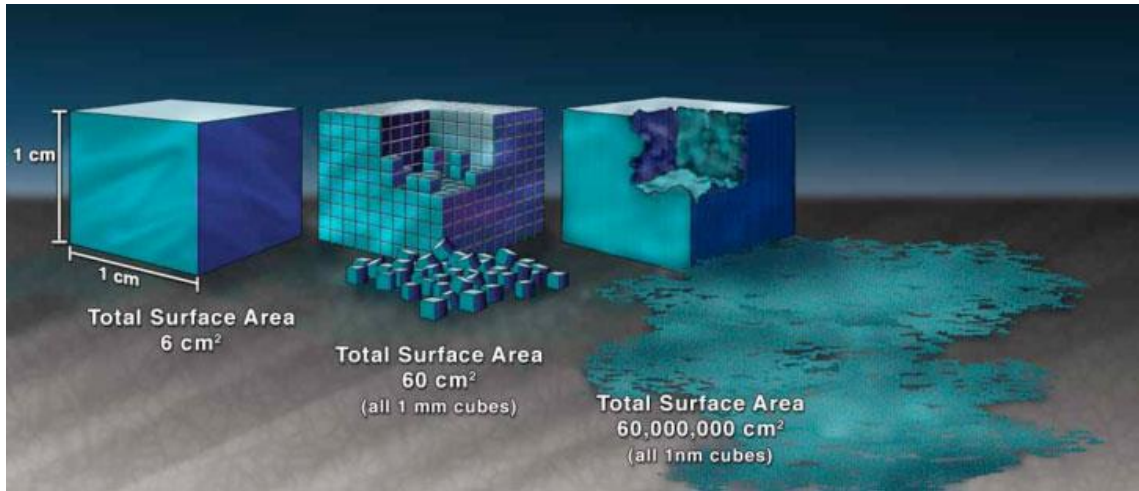
Figure 1.2 Comparison of surface area of same amount of material in different sizes [3].

There are wide electronic applications of nanotechnology as well as other fields such as medicine, food, fabrics, fuels, construction, biotechnology, energy etc. In the current technologies, flexible, wearable, bendable electronic devices are taking place of the traditional rigid and brittle materials. New application studies such as circuitries, displays, skin sensors, implantable medical devices, soft and human friendly wearable electronics, and highly deformable optoelectronic products [7,8] demand stretchable, transparent and conductive materials. This kind of materials should be durable against deforming operations in addition to having high conductivity and should conserve their properties and maintain the performance after these processes for a long time of use.

1.1. Transparent Conductors

Transparent electrodes are the most crucial component for electronic devices such as displays, touch panels, organic light emitting diodes (OLEDs), solar cells etc [9]. There are two important parameters while determining the performance of transparent electrodes. Transmittance (T) and sheet resistance (R_s) requirements depend on the type of device. For instance, while high T (>95%) values are necessary for high performance touch screens, they can tolerate 400-600 Ω sq^{-1} sheet resistance values. But for solar cells and large area displays, sheet resistance should be less than 20 Ω sq^{-1} in order to prevent voltage drops and heating during the device is working [10].

Indium tin oxide (ITO) is the most common material used as transparent electrode with over 90% transparency at 10 Ω sq^{-1} sheet resistance (on glass) [11], but it's brittle material and expensive because of the vacuum deposition process. In addition, the

reserves of ITO are decreasing [12]. These disadvantages triggered the researchers to find low-cost alternatives for transparent conducting electrode applications.

The most underresearched candidates to ITO are conducting polymers, carbon nanotubes (CNTs), graphene and metal nanostructures [12]. Individually, they have some limitations as a transparent conductor. For instance, to enhance the performance of carbon based nanomaterials, an expensive vacuum environment and a toxic chemical process is needed. Although conducting polymers are compatible for cost effective and large scale production, their conductivity is weak and requires extra processes to enhance the conductivity. Having excellent conductivity values makes 1D metallic nanowires the best alternative materials to ITO, however thermal annealing is needed to reduce junction resistance of nanowire network. Moreover, the conductivity performance and transparency of nanowire based conductors are affected by many parameters such as the size of nanowires [12]. In Table 1.1.1, some basic properties and fabrication methods for different transparent conductors are summarized.

Table 1.1.1 General properties and fabrication methods for different transparent conductive films such as transparent conductive oxides (TCOs), silver nanowire (AgNW), carbon nanotube (CNT), graphene and nanogrids [13,14].

Property	TCOs	AgNWs	CNT	Graphene	Nanogrids
R_s (Ω sq^{-1})	5- 100	1-50	60-300	30-5000	0.8
Tranmittance (%) (at 550 nm)	80-97	80-96	80-91	80-96	90
Flexibility	+	+++	+++	+++	+++
Stability	+++	+++	+++	+++	+++
Chemical Vapor deposition	+++	-	+	+++	+++
Sputtering	+++	-	-	-	+
Spray deposition	++	+++	+++	+	+++
Dip-coating	++	+++	+++	+	-
Screen printing	-	++	++	+	+++
Processing temperature (^{o}C)	>200[a]-1000	T_r-700[b]	T_r-700[b]	T_r-1000[b]	n/a
Cost	Low-High	Medium	High	High	Medium
Uniformity	+++	++	++	+++	+++

'+++' (high), '++' (medium), '+' (low), '-' (absent), n/a (no information)

[a] Deposition temperatures of TCOs usually require several hundred degrees Celsius or the use of vacuum processes such as sputtering.

[b] Networks can be fabricated at room temperature (T_r) but if device fabrication requires high temperature processes vacuum or encapsulation are required to stabilize the films.

Some of these disadvantages can be annihilated by using composite materials by taking advantages of individual materials. For example, one of the most studied composite material consists of AgNW and a conducting polymer, poly (3,4-ethylenedioxythiophene) polystyrene sulfonate (PEDOT:PSS). By using these two materials together, weak conductivity of polymer substrate and junction resistance of nanowire network were significantly enhanced without high temperature annealing process over 200 ºC by Lee et al. [12].

1.1.1. Indium Tin Oxide (ITO)

The main consumption field of indium element is the electrically conductive electrodes for flat panel displays, especially liquid crystal displays (LCDs) and touch screens as ITO thin-film coatings.

Abundance of indium is very low in the earth crust, estimated around 0.05 ppm [15]. In the Earth, indium is mostly found in zinc-sulfide ore mineral sphalerite and recovered from this source in the range of 1-100 ppm. Indium can also be found in some other metal-sulfides, but these sources are not economically favorable due to the trace amounts of indium. Because of its limited sources, the cost of indium is high, changing around $600 kg^{-1}. Annual refinery production of indium in different countries is given in Table 1.1.1.1. The leader manufacturer countries for indium are China and South Korea with production quantities of 410 and 150 tons in 2013, respectively [16].

Table 1.1.1.1 Annual production of indium in 2012 and 2013 [16].

	Refinery Production (tons)	
	2012	2013
United States	-	-
Belgium	30	30
Canada	62	65
China	405	410
Japan	71	71
Korea, Republic of	165	150
Peru	11	10
Russia	13	13
Other Countries	25	25
World total (rounded)	**782**	**770**

Indium tin oxide (ITO) is the most commonly used material with a 93% of all transparent conductor market. Its sale was about $1.6 billion in 2013 [11]. Although its high transmittance over 90 % at very low sheet resistances around 10 Ω sq^{-1} on glass, ITO has many unfavorable properties for transparent electrodes coming from its ceramic nature. Firstly, ITO is brittle and not a durable material to fracture. The other most important concern about the use of ITO is cost. High cost of ITO isn't only caused by the high cost of indium but also comes from high preparation temperatures and the slow, vapor phase sputtering process [11]. Because of these inadequate properties of ITO for new, flexible, transparent display technologies, there is a seeking for new alternative conducting materials to ITO.

1.1.2. Other Transparent Conductors

Various nanomaterials have been searched to meet the requirements as stretchable conductors and the most popular candidates are shown in Figure 1.1.2.1 [17]. Carbon nanomaterials have been one of the main research topics in new generation technologies. Nevertheless, they could be established in very limited applications as a result of their insufficient conductivity performance and high cost of carbon-based nanomaterials [8]. Among these materials, metal nanowires are the most promising alternative which meets the requirements to take place of ITO.
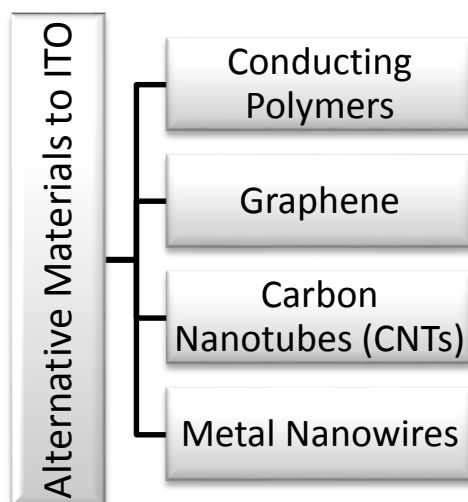
Figure 1.1.2.1 Alternative materials to ITO.

1.1.2.1. Conducting Polymers

Conducting polymers have been studied as alternative materials to ITO due to their superior properties such as easy solution process for production and various coating and printing techniques. The most commonly used polymer is PEDOT:PSS [17] – a macromolecular salt. As it's seen from the chemical structure of the polymer showed in Figure 1.1.2.1.1, it consists of two components. One component is poly (3,4-ethylenedioxythiophene)-PEDOT which carries positive charges and the other component is sulfonated polystyrene carrying negative charges [18]. PSS is also used to enhance the solubility of PEDOT in aqueous medium and balance the positive charges during polymerization reaction [17].
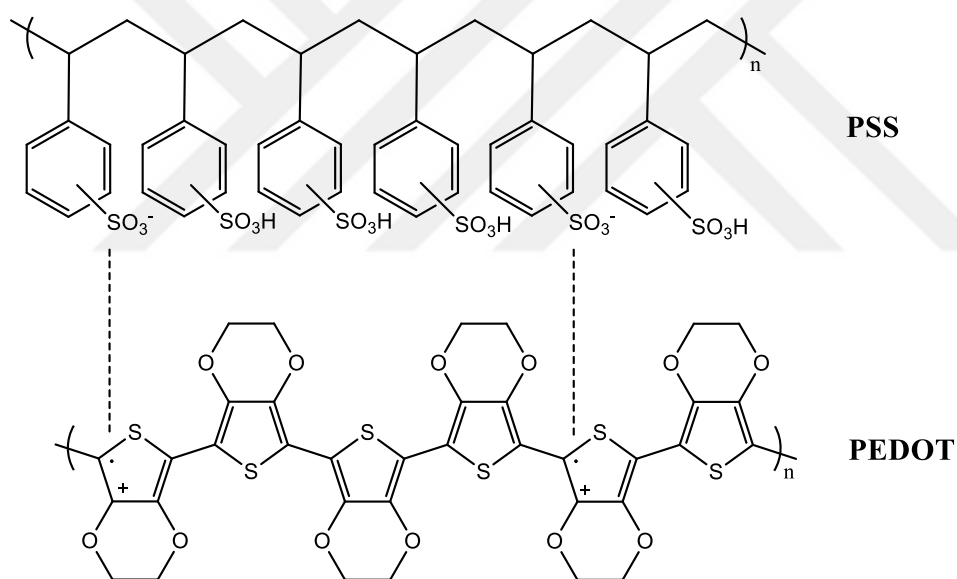
Figure 1.1.2.1.1 Chemical structure of PEDOT:PSS polymer.
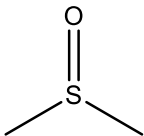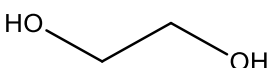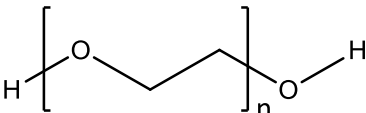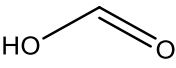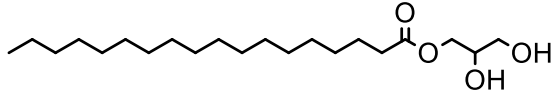
There are various processes suitable to fabricate thin films of PEDOT:PSS such as spin coating, bar coating, inkjet printing, and stamping printing. These solution based methods are simple and cheap. This can be count as an advantage of PEDOT:PSS applications [19]. On the other hand, conductivity of this polymer is typically around 1-10 S cm^{-1}, which is very low compared to conductivity of ITO (over 4000 S cm^{-1}) at similar transmission value (80%) [17] and at high transmittance values (>90%) the sheet resistance values reaches to >100 Ω sq^{-1} [11]. Conductivity value can be improved by

the increasing the thickness of polymer film, but this time transmittance of the polymer will be affected in a negative way according to the Beer-Lambert Law.

Conductivity of PEDOT:PSS can also be improved by the addition of high boiling point polar solvents such as ethylene glycol, sorbitol, dimethylsulfoxide (DMSO), glycerol, methylpyrrolidone, and other solvents given in Table 1.1.2.1.1, and by using different chemical methods to control the side groups of the polymer [17]. Although there are current commercial PEDOT:PSS products with high conductivity such as 850 S cm^{-1}, these values are still not comparable with ITO, which shows that this polymer is not a good material enough to replace with ITO alone.

Conductivity of polymer films could be increased with some post-treatments. Massonnet et. al. achieved 2273 S cm^{-1} conductivity without changing the crystalline structure by treating poly (3,4-ethylenedioxythiophene) trifluoromethanesulfonate (PEDOT:OTf) with H_2SO_4 [20]. For crystalline PEDOT:PSS nanofibrils, Kim and coworkers provided 4380 S cm^{-1} electrical conductivity by a structural rearrangement with H_2SO_4 treatment. After treatment they obtained highly ordered PEDOT:PSS nanofibrils which showed 90% transmittance at 46 Ω sq^{-1} sheet resistance as electrode [21].

Table 1.1.2.1.1 Summary of polar solvent additives for improving the electrical conductivity of PEDOT:PSS [19].

Polar solvent additive	Chemical structure	Max. electrical conductivity (S/cm)
Dimethyl sulfoxide		526 (Clevios PH510)
Ethylene glycol		1418 (Clevios PH1000)
Polyethylene glycol		805 (Clevios PH1000)
Formic acid		2050 (Clevios PH1000)
Glycerol monostearate		1019 (Clevios PH1000)

Clevios PH510-Specific conductivity=300 S cm^{-1}
Clevios PH1000-Specific conductivity=850 S cm^{-1}

1.1.2.2. Graphene

Graphene is an allotrope of carbon, which consists of carbon atoms oriented as a hexagonal lattice, forming two-dimensional structure. Graphene shows some surprising properties such as high strength, thermal and electrical conductivity and transparency [22]. These properties made graphene an alternative candidate for transparent conductor.
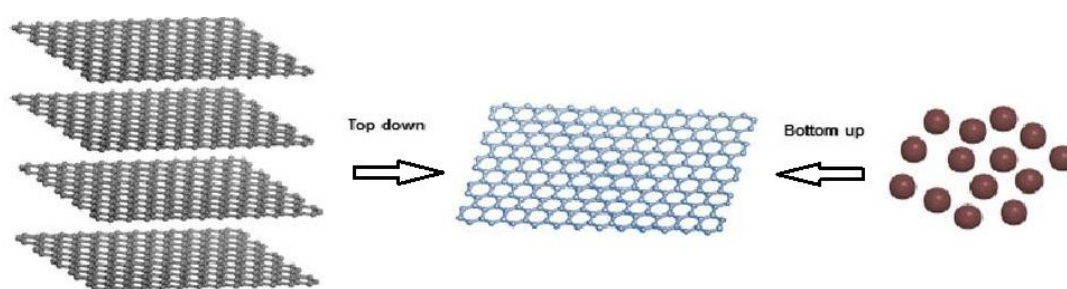
Figure 1.1.2.2.1 Schematic illustration of bottom-up and top down synthesis methods for graphene [23].

There are several methods reported by researchers for the production of different quality and featured graphene. These methods can be generally classified into two main topics: bottom-up and top-down synthesis as illustrated in Figure 1.1.2.2.1. Top-down methods focuses on obtaining graphene by breaking some sources such as graphite and graphite oxide (GO) into layers. Although top-down approaches, such as shearing, offers an easy and scalable production industrially, this kind of synthesis methods has some challenges such as surface defects in product-caused by sheet separation process and agglomeration of graphene sheets subsequently. In addition, obtained films after solution phase coating of graphene, which is produced by these low cost processes such as exfoliating graphite, shows poor performance in terms of transmittance and resistance (80% transmittance at 10 kΩ sq^{-1}) [11]. So it is hard to provide essential requirements of flexible, high conducting transparent electrodes with these methods [23].

In bottom up approaches, graphene is constructed by using carbon molecules as building blocks obtained from alternative sources. The leading bottom-up technique for thin graphene film synthesis is chemical vapor deposition (CVD). Although high quality and well thickness controlled large size of graphene films can be produced which are appropriate for the use in touch screens, smart windows, solar cells, flexible LCD, and

OLEDs by this technique, being incompatible for industrialization due to its high cost and high operating temperature (1000 ºC) [11] are big obstacles for this method [23].

1.1.2.3. Carbon Nanotubes (CNTs)

Carbon nanotube (CNT) is an allotrope of carbon with an extraordinary length/diameter ratio up to 132,000,000 [19]. They show similar chemical and physical features to graphene such as good conductivity, transparency, outstanding flexibility coming from their same hexagonal honeycomb carbon lattice unit. But they differ in geometrical structures. A single walled carbon nanotube (SWCNT) can be considered to be formed by rolling up a graphene sheet along a vector [24].

There are many advantages of carbon based nanomaterials. Owing to the abundance of carbon, CNTs and graphene are able to meet the demand of transparent electrode market. Their high flexibility is also another attractive property for new generation flexible devices. Other excellent properties of CNTs, including high mechanical strength, thermal and electrical conductivity, wide transmittance spectrum range, durability and compatibility with solution phase coating processes make them to be considered a good alternative to ITO [11,17]. Also the mass-production of CNTs is possible with relatively low costs which make CNTs an attractive material for transparent conductors.

There are various methods to synthesize CNTs such as arc discharge, laser ablation, and CVD [25]. CNT-based transparent conductors typically show 400 Ω sq^{-1} sheet resistance at 90 % transmittance. This high resistance value originates from the contact points of CNTs [11]. Hecht and coworkers could reduce the sheet resistance of CNT film to 60 Ω sq^{-1} at 90.9 % transmittance by doping with chlorosulfonic superacid and obtained the best performance for CNT films which also surpassed the performance of PEDOT:PSS [11].

1.1.2.4. Metal Nanowire Network

When the subject comes to conductivity, metals are always the first material type coming to the mind due to their high free-electron densities. Seeking new materials for transparent conductor applications as a result of the economic and physical

disadvantages of ITO for low cost applications drew great attention on metals as a good alternative. With this concern, researchers dwelled on ultra-thin metal layers and metal nanowires as potential materials [17]. When metal films are thin enough (<10 nm), they become transparent under visible light. On the other hand, having small thickness can cause poor electrical conductivity because of the discontinuity of film [26]. Studies showed that ultra-thin metal layers are not suitable materials for transparent electrodes due to its high surface scattering of free charge carriers. Having a thickness smaller than the mean free path length causes a great increase in the film resistivity. Sheet resistance can be reduced by increase in thickness, but this time material becomes unsuitable in terms of transparency. For example, ultra-thin Ag films usually exhibit low transmission around 60 % at a thickness of 10 nm [17]. Metals show more promising results as transparent conductors when they are applied as dispersed random nanowire networks.

Metallic nanowires have drawn remarkable attention in the past decade and been the focus of many researchers due to their excellent mechanical, electrical, thermal and catalytic properties which are crucial for many applications. In addition to these excellent properties, having low manufacturing cost and being suitable for solution deposited roll-to roll techniques are other advantages of studying with nanowires [26].

In order to make a device in which nanowires are used as conducting materials, nanowires should provide some parameter such as high oxidation resistance, high aspect ratio (L/D), high purity, and good dispersibility [7]. To gain stretchability to a device is a challenging process as in making foldable and bendable electronics. Having short lengths (1-20 μm) for 1D metal nanowire networks can cause deterioration in electrical conductivity and mechanical durability [8]. From this point of view, some researches brought solutions to stretchability problem by synthesis and use of longer nanowires in electronics. During the development of conductors with metal nanowires, high aspect ratio of NWs is critical for both high electrical conductivity and mechanical compliance since it is difficult to provide both properties to a device at the same time [8].

When working with nanowire network for transparent conductor applications, one of the main obstacle is high sheet resistance, especially arises from the junction points of nanowires. To eliminate this problem, different solutions for reducing junction resistance such as mechanical pressing, light induced plasmonic nanowelding and thermal annealing have been reported [27]. Langley et al. reported that for a silver nanowire network, consisted of nanowires with 105 nm in diameter and 37.5 μm in length, that the sheet resistance of the film had been reduced from 10^7 Ω sq^{-1} to 9.5 Ω

sq^{-1} at 90% transmittance by thermal annealing process at 200 °C for 2 hours [27]. Another method to reduce the sheet resistance is using a composite film which consists of metal nanowires and conducting polymer as illustrated in Figure 1.1.2.4.1. Lee et al. achieved to fabricate hybrid conducting film of very long silver nanowires (AgNWs) and PEDOT:PSS by this nanosoldering approach with 25-54 Ω sq^{-1} at 90% transmittance value [12].
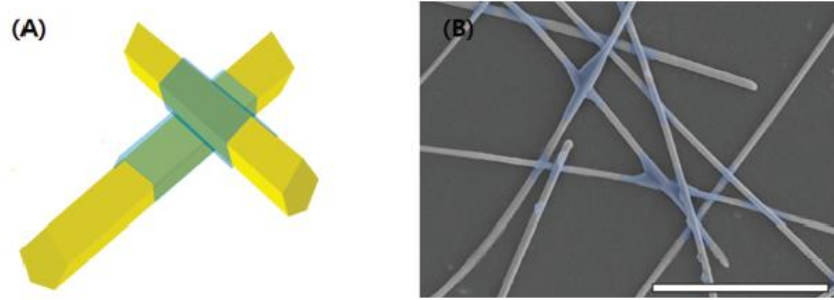
Figure 1.1.2.4.1 Illustration and SEM image of room temperature AgNW nanosoldering by PEDOT:PSS assisted joining at the nanowire junctions. The inset scale bar is 4 μm [12].

As stretchable transparent conductors, silver and copper nanowires are the most remarkable ones among the metals due to their high conductivities. Conductivity data of common metals and other materials are given in Table 1.1.2.4.1.

Table 1.1.2.4.1 Conductivity of materials [28].

Material	ρ (Ω•m) at 20 °C Resistivity	σ (S/m) at 20 °C Conductivity	Material	ρ (Ω•m) at 20 °C Resistivity	σ (S/m) at 20 °C Conductivity
Silver	1.59×10^{-8}	6.30×10^{7}	Stainless steel	6.9×10^{-7}	1.45×10^{6}
Copper	1.68×10^{-8}	5.96×10^{7}	Mercury	9.8×10^{-7}	1.02×10^{6}
Gold	2.44×10^{-8}	4.10×10^{7}	Nichrome	1.10×10^{-6}	9.09×10^{5}
Aluminum	2.82×10^{-8}	3.5×10^{7}	GaAs	5×10^{-7} to 10×10^{-3}	5×10^{-8} to 10^{3}
Calcium	3.36×10^{-8}	2.98×10^{7}	Carbon (amorphous)	5×10^{-4} to 8×10^{-4}	1.25 to 2×10^{3}
Tungsten	5.60×10^{-8}	1.79×10^{7}	Carbon (graphite)	$\sim10^{-6}$ //basal plane $\sim10^{-3}$ ⊥basal plane	$\sim10^{5}$ //basal plane $\sim10^{2}$ ⊥basal plane
Zinc	5.90×10^{-8}	1.69×10^{7}	Germanium	4.6×10^{-1}	2.17
Nickel	6.99×10^{-8}	1.43×10^{7}	Sea water	2×10^{-1}	4.8
Lithium	9.28×10^{-8}	1.08×10^{7}	Drinking water	2×10^{1} to 2×10^{3}	5×10^{-4} to 5×10^{-2}
Iron	1.0×10^{-7}	1.00×10^{7}	Silicon	6.40×10^{2}	1.56×10^{-3}
Platinum	1.06×10^{-7}	9.43×10^{6}	DI water	1.8×10^{5}	5.5×10^{-6}
Tin	1.09×10^{-7}	9.17×10^{6}	Glass	10×10^{10} to 10×10^{14}	10^{-11} to 10^{-15}
Carbon steel	(10^{10})	1.43×10^{-7}	Air	1.3×10^{16} to 3.3×10^{16}	3×10^{-15} to 8×10^{-15}
Lead	2.2×10^{-7}	4.55×10^{6}	PET	10×10^{20}	10^{-21}
Titanium	4.20×10^{-7}	2.38×10^{6}	Teflon	10×10^{22} to 10×10^{24}	10^{-25} to 10^{-23}

1.2. Environmental Problems-Dye Waste Water

There are wide applications of organic dyes industrially such as textile, paper, color photography, pharmaceutical, food, cosmetic, electric etc. Every year there is dye production over 0.7 million tons [29] which means a large amount of wastewater that causes water pollution resulting with hazardous effects on aquatic ecosystems and serious impacts on health. These organic dyes are visible even in very low concentrations. When they are drained into water sources as seen in Figure 1.2.1, they affect the bacterial growth negatively by causing adsorption or reflection of the sunlight. Furthermore, because they usually are toxic and carcinogenic, they harm aquatic life and damage food chain [29].

There are physical, chemical and biological methods for industrial wastewater treatment. Physical treatment methods such as filtration, sedimentation, adsorption, and coagulation/flocculation include only physical and mechanical processes. By these methods, waste materials cannot be transformed into nonhazardous species chemically. Furthermore, physical treatments are not effective for the waste which is in liquid or dissolved form like dyes. In the most common chemical treatment methods, chlorine, ozone, and potassium permanganate are used to provide the electron transfer which the chemical treatments are based on. Although these methods are effective, there are also some important disadvantages. For example, when chlorine is used, chlorinated hydrocarbons, which can be more toxic and carcinogenic than the waste itself, can be produced. For this reason some countries imposed restriction for the use of chlorine. Ozone and permanganate usage are expensive methods and removal of precipitation of manganese oxide is a big problem after treatment. However biological treatments are more advantageous than physical and chemical methods in terms of being more economic and simpler, for the wastewater of dye industries, the application of these methods are not successful due to low biodegradability of organic dyes [30].

These methods are not efficient enough to decolorize the dyes [31], in other words not enough to annihilate the hazardous effects of dyes on nature. Due to the limitations of these traditional wastewater technologies, advanced oxidation processes (AOPs), which are based on decolorization and reduction of wastewater by using highly reactive

chemicals such as hydroxyl radicals, were suggested [30]. Although AOPs are efficient and don't create waste much, they are expensive methods, too.

Figure 1.2.1 Dye pollution from textile plants is a source of environmental concern in China [32].

Chapter 2

Silver Nanowire

2.1. Literature Survey

2.1.1. Silver Nanowire Transparent Conductors

Silver is the most electrically conductive material as it's seen in Table 1.1.2.4.1. This property gives silver a great potential of being a good alternative for transparent conductors. This advantage of silver has been taken by many researchers and silver studied in nanowire form for transparent conductors.

The most common method to synthesize silver nanowires (AgNWs) is the reduction of silver nitrate ($AgNO_3$) by ethylene glycol (EG) in the presence of polyvinylpyrrolidone (PVP). The synthesized nanowires are usually~ 40-200 nm in diameter and 1-20 µm in length, in the literature [26].

Although silver nanowire is very good material as transparent conductor due to its high conductivity, there is still some obstacles, such as high sheet resistance caused by contact points of nanowires, high haze levels and oxidation, needed to be annihilated before being used for this kind of application. Thermal annealing is one of the methods to reduce the sheet resistance of conducting films. After deposition of the silver nanowires to prepare a film, PVP residues on nanowires hinder the electrical conduction and cause a high sheet resistance. It was shown that AgNW network exhibits the minimum electrical resistance for an annealing temperature changing from 200 to 320 ºC by Langley and coworkers [27]. They could obtain 90% transmittance and 9.5 Ω sq^{-1} resistance with an annealing period of 2 h at 200 ºC. Lee et. al also proved that annealing at 220 ºC for 2 h, electrical properties of the film were improved significantly by removing PVP residues and nanowelding at the junction points [8]. In order to

reduce the annealing temperature, Kim and coworkers used polycarbonate (PC) substrate [33]. After electrostatic spray deposition of AgNWs on the substrate, they applied annealing process at 120 ºC for 8 h and obtained a conducting film showing 92.1% transmittance at 20 Ω sq^{-1} resistivity. Hu et al. reported another solution to prevent high resistance [26]. As they showed, mechanical pressing and electroplating of metal can also result with a dramatic decrease of the sheet resistance and surface roughness, which is another problem for applications with thin active layers. In Figure 2.1.1.1, SEM images of a comparison study for thermally annealed and mechanically pressed silver nanowire networks are shown [34].
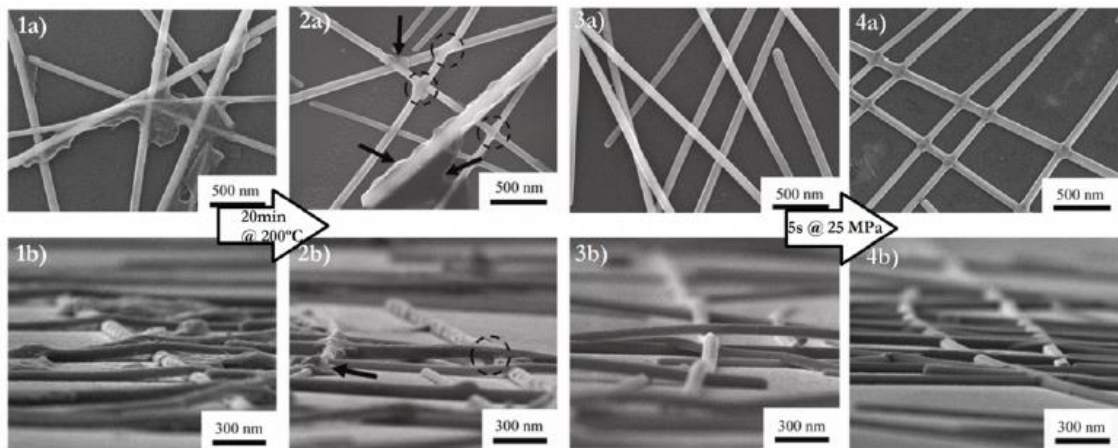
Figure 2.1.1.1 SEM images of AgNW networks, the **(a)** series are top-down views of the sample and the **(b)** series show off-angle cross-sectional views. Images 1(a) and (b) are of as-deposited nanowire networks. 2(a) and (b) show the effect of thermal annealing at 200 ºC for 20 min. 3(a) and (b) show an as-deposited network after rinsing in water and ethanol and 4(a) and (b) show the effect of 5 s of mechanical pressure applied at 25 MPa [34].

Metallic character of these films causes some problems in terms of transmittance of light. Some of the light is reflected from the surface of metals. Especially silver leads high light scattering which is known as haze, reason for blurriness, and this is not desirable for many display applications. Because light scattering is directly proportional to surface roughness, methods such as thermal annealing and mechanical pressing, which reduce the roughness, can be used to decrease the haze of silver nanowire films.

Surface roughness is not the only reason for high haze levels. When the metal surface is big, amount of scattered light will also be high, so will the haze. So theoretically, using nanowires with smaller diameters would decrease the haze and using longer nanowires would decrease the junction points by decreasing the number of nanowires used which results in a drop of sheet resistance value.

Ultra long silver nanowires are also suitable materials in terms of stretchability. Lee et al. used silver nanowires, over 500 μm in length and synthesized by successive multistep growth, to make a stretchable electrode by transferring the nanowire network on a highly stretchable polymer substrate. The electrode they fabricated showed 9-70 Ω sq^{-1} resistivity at 90-96% transmittance, and they achieved 460% strain and low sheet resistance, better values than related material in this field including carbon nanotubes and graphene [8]. Another transparent conductor application study with ultra-long silver nanowires showed that even after many cycling bending over 20,000 and 5-10 % stretching, the nanowires could maintain their electrical functionalities and stability with a low sheet resistance (25-54 Ω sq^{-1}) at 90% transmittance on a plastic substrate [12].

Oxidation is another problem for the lifetime of devices while using silver. Stability of the materials is very important for sustainability of the performance. Kim et al. showed that coating the surface of AgNWs with a gold layer protects the nanowires against oxidation and sulfurization according to sheet resistance measurements of AgNW electrode and Au coated AgNW electrode which were tested in the air at 80 $^{\circ}$C [35]. They reported that coating gold on the AgNW surfaces is also useful to enhance the optical properties of AgNW electrodes by reducing haze.

2.1.2. Silver Nanowire Synthesis Methods

There are various different reported methods for silver nanowire synthesis other than the polyol method such as UV irradiation, photo-reduction technique, electro-deposition process, DNA template method, porous material template method and wet chemical method [36].

The most used method for the synthesis of silver nanowires is the polyol method which was first developed by Fievet et. al. to synthesize colloidal metal particles such as Ag, Au, Cu, Ir, Ni, Pd, Pt, Ru, CoNi and FeNi [37]. The method is simply based on the reduction of noble metal salts by ethylene glycol (EG) at over 150 $^{\circ}$C in the presence of a shape directing polymer which forms a coordination complex with metal ions by selective absorbance onto surface of the metal. Different polymers were used to stabilize the metals and direct the growth such as polyvinylpyrrolidone (PVP), sodium dodecylulfonate (SDS), bitamin B$_2$, polyvinylalcohol (PVA) and dextrin. However, it

was proved by studies that PVP is the best stabilizing agent due to its high degree of polymerization among all other polymers [36].

Interaction between the oxygen and PVP molecule and {100} facet of Ag is proved to be stronger than the interaction between PVP and {111} facet by studies. Therefore, PVP molecules block {100} facet of Ag and the growth occurs on {111} facet. It was observed that AgNWs synthesized by polyol method have five folds twinned crystalline structure with a pentagonal cross sectional shape as illustrated in Figure 2.1.2.1 [36].
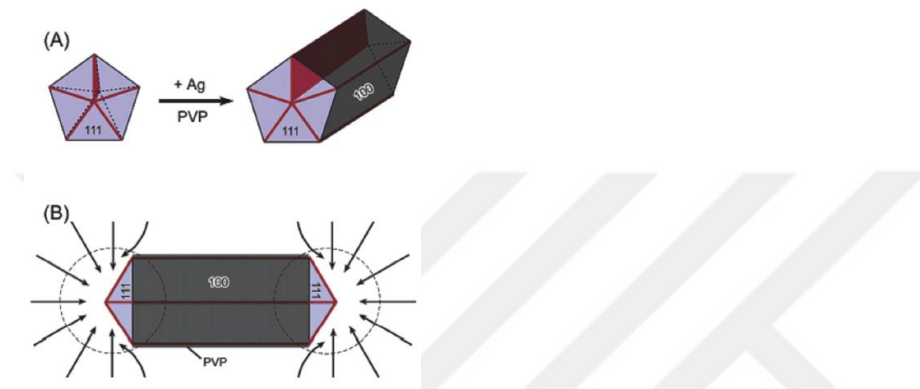
Figure 2.1.2.1 Growth mechanism of silver nanowires.

Polyol method is a solution based method and applied by Sun et al. to synthesize silver nanowires with 30-40 nm in diameter and lengths up to 50 μm [38]. In this process $AgNO_3$ was reduced by EG in the presence of PVP. At first, silver nanoparticles are formed from Ag^+ ions (Pt nanoparticles when Pt seeded process) by reduction at 160 ℃ and then grow in one dimension anisotropically by the help of PVP molecules as shown in Figure 2.1.2.2. In some studies, different sources were used to generate seeds for the AgNW growth, such as $CuCl_2$ [39].
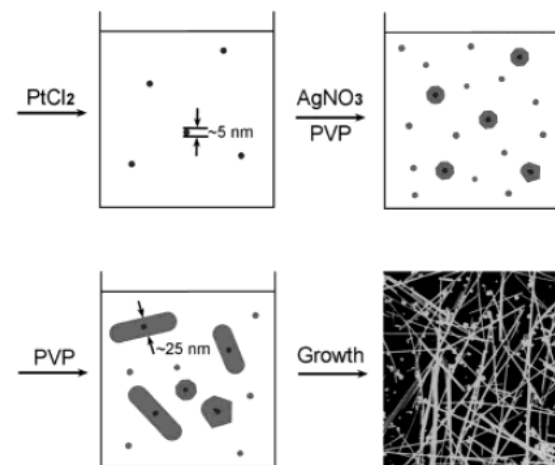
Figure 2.1.2.2 Schematic illustration of the experimental procedure that generates silver nanowires through a Pt-seeded polyol process [38].

18

Kim et al. used a modified polyol synthesis method by adding KBr and using NaCl instead of AgCl and obtained silver nanowires with 13.5 μm in length and 62.5 nm in diameter, averagely [33]. Addition of KBr before the AgNO$_3$ addition causes a competition between ions and results in a decrease in number of Ag$^+$ ions. This procedure was reported in many studies for the formation of longer and thinner nanowires. Kim and coworkers also used NaCl for seeding process instead of PtCl$_2$ or AgNO$_3$. By this modification they provide more controlled growth procedure for nanowire formation by eliminating the Ag sources in the solution before addition of AgNO$_3$ in one step.

There are other studies in which NaCl was used in seeding process, too. Coşkun et al. performed a parametric study for the silver nanowire synthesis with polyol method [40]. It was reported that there might also be a stabilizing effect of chloride ions (Cl$^-$) on silver nanoparticles which is preventing them from aggregation [41]. So the amount of NaCl is also important for the efficiency of the reaction and the structure of the product as well as the other factors such as PVP/AgNO$_3$ ratio, injection rates of reactants and stirring rate. By optimizing these parameters, Coşkun and coworkers could synthesize silver nanowires with 63 nm in diameter and 8.4 μm in length, averagely.

Temperature is another parameter which has a great effect on product structure in polyol synthesis. Xia et. al. claimed that when the reaction temperature is above 150 ºC, glycolaldehyde (GA) forms from EG in the presence of oxygen as it's shown below and the generated GA becomes the dominant reductant at these temperatures due to its stronger reductive property than EG. When the reduction reaction of AgNO$_3$ was performed in an atmosphere which O$_2$ was totally removed, they recorded that Ag$^+$ ions were still reduced but with a slower rate by EG [42]. Oxidation of EG to GA was shown below in reaction equation (2.1.2.1):

$$2HOCH_2CH_2OH + O_2 \xrightarrow{\Delta} 2HOCH_2CHO + 2H_2O \qquad (2.1.2.1)$$

The length of nanowires plays an important role to succeed good electrical conductivity and mechanical properties such as flexibility and stretchability in a metal nanowire network by providing more effective electron transfer with lower nanowire number compared to the shorter nanowires by decreasing the inter-nanowire junctions which have the most contribution to resistivity [8]. Through this approach, Lee et al. achieved to synthesize ultra-long AgNWs over 500 μm in length and 100-150 nm in

diameter by a multistep growth process as illustrated in Figure 2.1.2.3, that is repetitive AgNO$_3$ reduction in ethylene glycol (EG) solution with PVP under carefully controlled conditions [8]. By using these ultra-long AgNWs, they achieved 90-96% transparency and 9-70 ohm sq^{-1} resistivity which are superior values than other reported transparent conductors made from CNTs, graphene, ITO and short AgNWs.
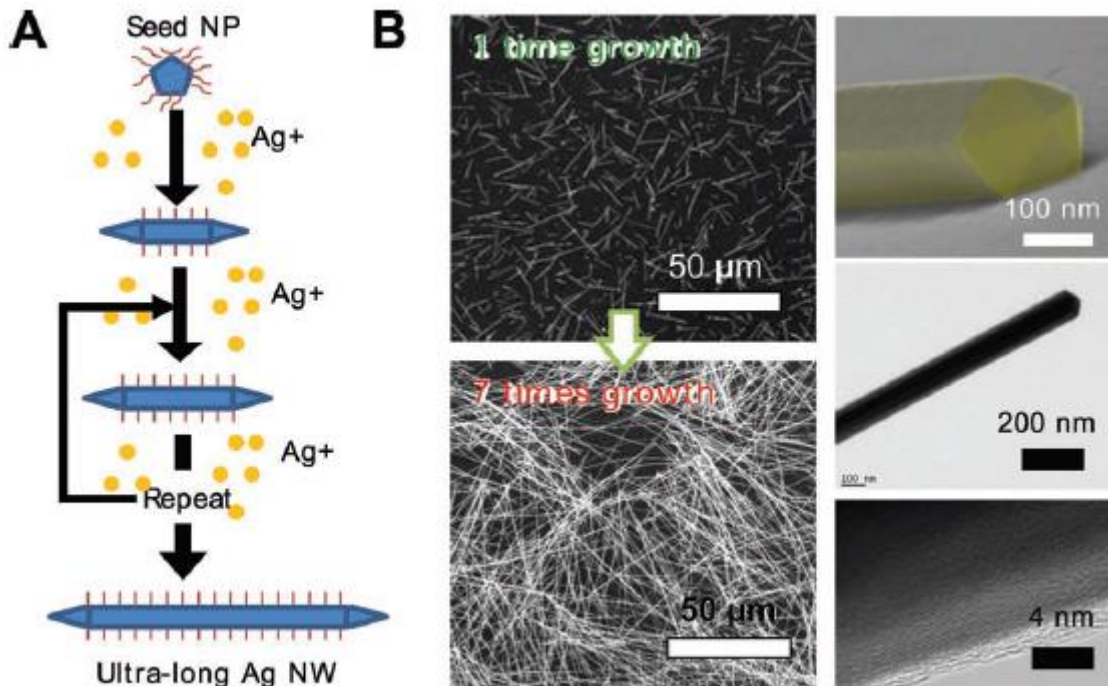
Figure 2.1.2.3 a) Synthesis processes of very long AgNWs through multi step growth process. **b)** SEM images of AgNWs after 1 and 7 times growth. SEM and high resolution TEM images of an individual Ag NW after a 7 times process [8].

2.1.3. Coating Studies of AgNWs with Noble Metals

Surface of silver nanowires can be modified via coating with different materials for different purposes. For example, SiO$_2$ was successfully coated on silver nanowires via Stöber method-a sol-gel approach by Xia and coworkers [43]. These Ag@SiO$_2$ core-shell nanocables can be used as connectors in nanoscale devices. Catalyst features can also be gained by using an appropriate precursor for coating. Sun et al. synthesized a catalyst by replacing the surface atoms of silver nanowire with AgCl [44].

Silver is sensitive to oxidation under air conditions which is undesirable for silver nanowire based transparent conductors. On the purpose of preventing this problem, nanowire surfaces can also be coated with other noble metals. Kim et al., used a gold

complex, [Au(en)$_2$]Cl$_3$, and reported that homogeneous gold layer coating on silver nanowires with controllable thickness were succeeded via galvanic exchange due to lower reduction potential between gold complex and silver compared to the case with HAuCl$_4$ [35].

In this study, galvanic exchange reactions between silver nanowires and other nobel metals, Pd and Pt, was performed in order to change the surface properties and prevent oxidation.

2.2. Experimental Section

2.2.1. Synthesis of Silver Nanowire

2.2.1.1. Materials

Ethylene glycol (EG, $\geq$99%, Sigma-Aldrich), silver nitrate (AgNO$_3$, $\geq$99.0%, Sigma-Aldrich), polyvinylpyrrolidone (PVP) (average MW of 10000, PVP10, Sigma-Aldrich), PVP (average MW of 40000, PVP40, Sigma-Aldrich), PVP (average MW of 360000, PVP360, Sigma-Aldrich), NaCl ($\geq$99.8%, Sigma-Aldrich) and KBr ($\geq$99.5%, Merck) were used in the synthesis of silver nanowires.

2.2.1.2. Synthesis Procedure

Silver nanowires were synthesized by polyol method which is based on the reduction of AgNO$_3$ by ethylene glycol in the presence of PVP that is used as the capping agent. After dissolution of PVP in 25 ml of ethylene glycol (quantity details were included in Table 2.2.1.2.1), the solution was heated up in oil bath with an optimized temperature of 170 ºC. Subsequently, 0.05 g of NaCl and 0.025 g of KBr salts were added to the solution and the solution was kept stirred at 400 rpm. After waiting for the dissolution of salts for a few minutes, finely grained 2 mmol of AgNO$_3$ was added rapidly to the solution. The reactions were carried out at this fixed temperature for different time intervals which were optimized as 3 h for PVP40 and PVP360 and 45 min for PVP10. After reaction completed, solution was cooled down to

the room temperature and washed with methanol by using glass filter (POR.3). After filtration, the solution was rested for one day and particles accumulated at the bottom were removed from the solution.

Table 2.2.1.2.1 Amount of PVP in different PVP/AgNO$_3$ ratios dissolved in 25 ml EG.

PVP/AgNO$_3$ molar ratio	PVP10 (g)	PVP40 (g)	PVP360 (g)
0.5 k	-	-	1.0286
1.5 k	-	0.3429	3.0857
2.5 k	0.1429	0.5714	-
3.5 k	0.2000	0.8000	-
4.5 k	0.2571	1.0286	-
5.5 k	0.3143	1.2571	-
6.5 k	-	1.4857	-

*k=2.78x10^{-3}

2.2.2. Coating of Silver Nanowires With Noble Metals

Different methods were tried to be applied to coat the surface of silver nanowires with noble metals such as Au, Pd, and Pt.

Au coating on silver nanowires was performed by using HAuCl$_4$ as gold precursor through following process [45]. Different volume (2.7 ml, 4.41 ml, 8.11 ml, 10.82 ml, 13.52 ml, and 16.22 ml) of 0.25 mM HAuCl$_4$ was added into 20 ml of diluted AgNW solution, which was prepared by addition of 19 ml methanol into 1 ml AgNW (3.5 mg/ml) solution, at 65 °C. 30 min after HAuCl$_4$ addition, reaction was finished and final solution was cooled down to the room temperature before washing with methanol a few times.

For Pd coating on silver nanowires, PdCl$_2$ was used as Pd precursor through following process [46]. A palladium solution was prepared by addition of 1.7 mg PdCl$_2$ into PVP-EG solution (34.193 mg PVP 40, 5.6989 ml EG). Then 8 ml AgNW solution (2.6 mg/ml) was dissolved in 20 ml EG in a different flask. Next, prepared Pd solution was added into AgNW solution and the medium was filled with N$_2$ (g). Temperature of the resulting solution was increased to 90 °C. After 2 h, solution was cooled down to the

room temperature. Final solution was washed with methanol a few times to remove EG. This process was performed with the half amount of $PdCl_2$, too.

For Pt coating on silver nanowires, H_2Cl_6Pt was used as Pt precursor as explained in following process [45]. 2 ml of AgNW solution (3.5 mg/ml) was diluted to 20 ml by methanol and the diluted solution was heated up to 65 ºC in an oil bath. Then 5 ml H_2Cl_6Pt solution (1 mM) was added drop by drop while stirring. After addition of Pt solution, the solution was left to cool down and then the product washed with methanol a few times by using centrifugation. The final product was stored in methanol.

Au, Pd and Pt coatings were also performed by using complex solutions of these metals ($[Au(en)_2]Cl_3$, $[Pd(en)_2]Cl_2$, $[Pt(en)_2]Cl_2$) to achieve milder reaction rates [35]: These noble metal complexes were used to coat AgNW surface by using two different methods: direct addition drop by drop and biphasic coating.

In direct addition method, 4 ml of AgNW solution (1 mg/ml) was diluted to 20 ml by deionized water and the diluted solution was heated up to 90-95 ºC in an oil bath. Then 20.4 ml complex solution (0.25 mM) was added drop by drop while stirring. 20 ml NH_3 solution was also added to remove AgCl. After addition of complex, the solution was left to cool down and then the product washed with methanol a few times by using centrifugation. The final product was stored in methanol.

In biphasic method, 1 ml of AgNW solution (1 mg/ml) was diluted to 20 ml by deionized water and 20 ml ethyl acetate was added to the solution. The flask was heated up to 90-95 ºC while stirring. Then 5.1 ml of complex solution (0.25 mM) was added slowly. During the addition of complex solution, 5 ml NH_3 was also introduced to the flask. After cooling down, the same washing process was applied and the product was stored in methanol. This method was also performed with 5.1 ml and 2.5 ml $HAuCl_4$, too.

2.3. Characterization

2.3.1. Scanning Electron Microscope (SEM)

Surface morphology and size of nanowires were determined by LEO 440 scanning electron microscopy (SEM).

2.3.2. Energy Dispersive X-Ray Spectroscopy (EDX)

Energy dispersive X-ray spectroscopy (EDX) was used to understand the composition of copper nanowires

2.4. Result and Discussion

2.4.1. Characterization of Silver Nanowires

In this modified polyol synthesis method, the most important differences between classical polyol method are using only $AgNO_3$ as Ag sources and addition of NaCl as source of Cl^- ion which has an important role for the stabilization of Ag nanoparticles (seeds) and nanowires.

With the intent to understand how PVP molecule size affects the silver nanowire formation, three different PVP molecules were used as capping agents. Synthesis reactions were performed with PVP10, PVP40 and PVP360 with different $PVP/AgNO_3$ ratios and the products were characterized by SEM.

Results showed us that reaction yield for silver nanowire formation is not high when PVP 10 is used. Figure 2.4.1.1 shows the SEM images of products in the presence of PVP 10 as capping agent. In order to observe the effect of PVP amount, synthesis reaction was performed with different $PVP/AgNO_3$ molar ratios. Table 2.4.1.1 shows the size data of obtained AgNWs. Changing the ratio didn't affect the length of nanowires prominently, but significant decrease in diameter of nanowires was observed at higher ratios and it results with higher aspect ratio. In this reaction, rod shape

24

products and big particles were also formed in addition to nanowires. There is also big difference in diameters among nanowires. So we can say that short size PVP molecules are not efficient enough to prevent the growth on nanowire surface, especially in low quantities. This outcome is not favorable for the use of nanowires in display applications.
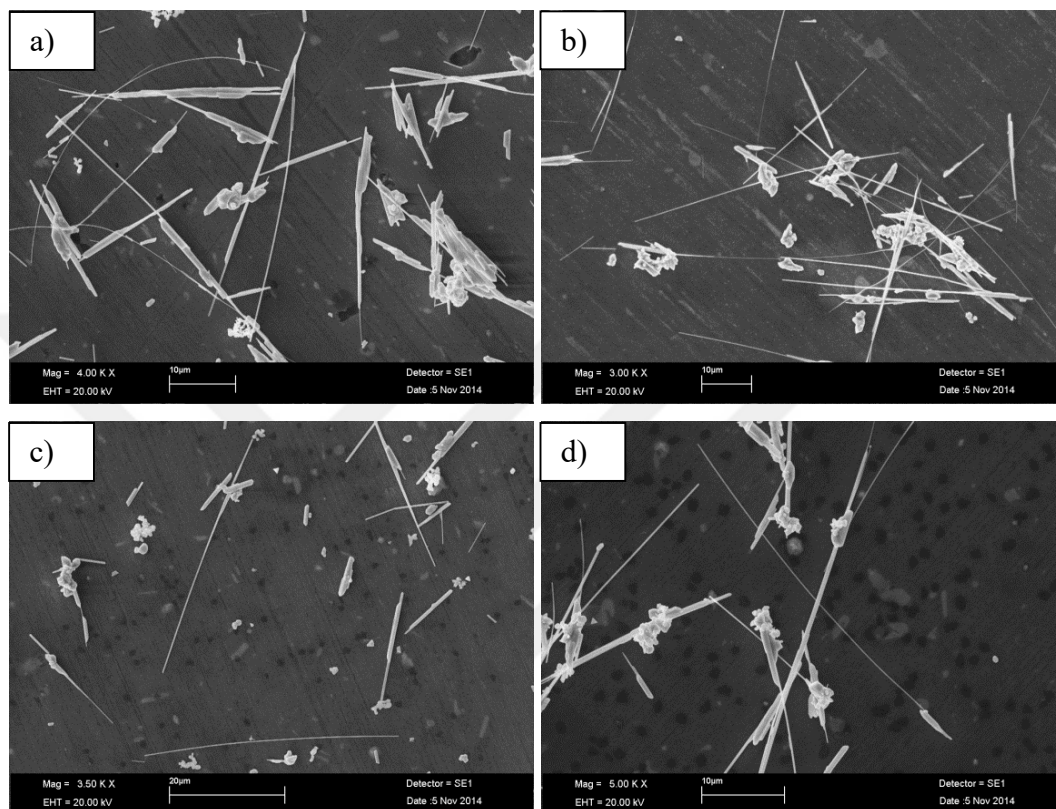
Figure 2.4.1.1 SEM images of silver nanowires with PVP 10/AgNO$_3$ ratio of **a)** 2.5k, **b)** 3.5k, **c)** 4.5k and **d)** 5.5k.

Table 2.4.1.1 Average length and diameter data of AgNWs synthesized with PVP10.

PVP/AgNO$_3$ molar ratio	Length (μm)	Diameter (nm)	L/D
2.5k	42	230	183
3.5k	37	200	185
4.5k	48	125	381
5.5k	47	137	344

*k=2.78x10^{-3}

As it is seen in Figure 2.4.1.2, nanowires synthesized by using PVP40 as shape directing agent are very clear and homogeneous structures for all molar ratios of PVP and $AgNO_3$ compared to the product obtained by using PVP10.
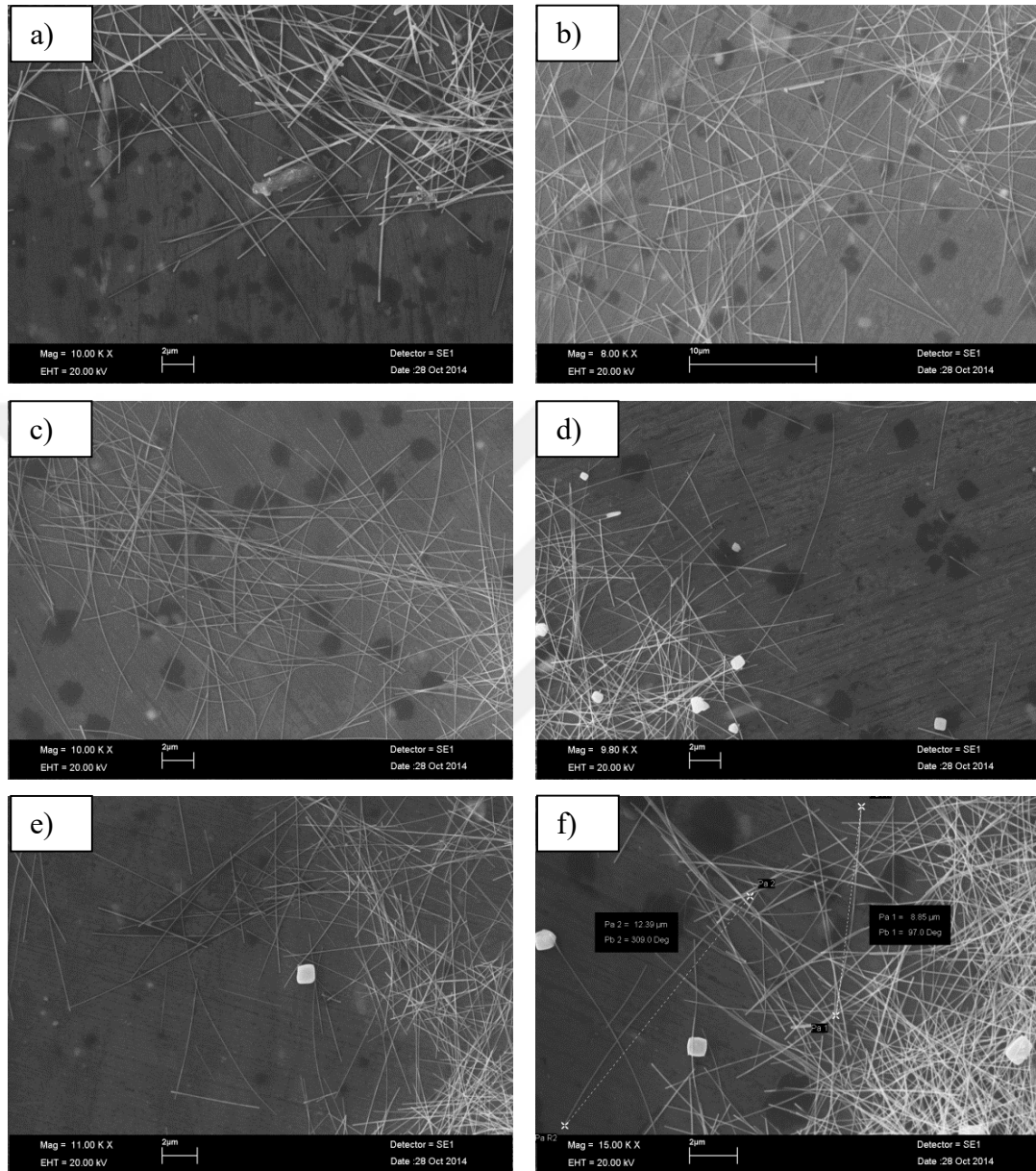
Figure 2.4.1.2 SEM images of silver nanowires with PVP40/$AgNO_3$ ratio of **a)** 1.5k, **b)** 2.5k, **c)** 3.5k **d)** 4.5k, **e)** 5.5k and **f)** 6.5k.

Table 2.4.1.2 gives the average sizes of nanowires synthesized with PVP40. Nanowires with the lowest diameter were obtained in the 3.5k molar ratio. Very low and high ratio values ended up with a decrease in nanowire length. The average diameter of nanowires is also high at 1.5k. We can say that in this ratio, amount of PVP molecule couldn't prevent the growth on the surface.

Table 2.4.1.2 Length and diameter data of AgNWs synthesized with PVP40.

PVP/AgNO$_3$ molar ratio	Length (μm)	Diameter (nm)	L/D
1.5k	17	70	240
2.5k	25	48	525
3.5k	21	35	615
4.5k	21	65	325
5.5k	17	53	320
6.5k	10	47	220

*k=2.78x10^{-3}

By using PVP360, very clear products were obtained, too, as it's seen in Figure 2.4.1.3. Obtained size data are shown in Table 2.4.1.3. With the increase in molar ratio, not only the length of nanowires increased but also the diameters. Higher PVP quantities couldn't be studied due to the solubility problems of PVP molecules in EG in high amounts.
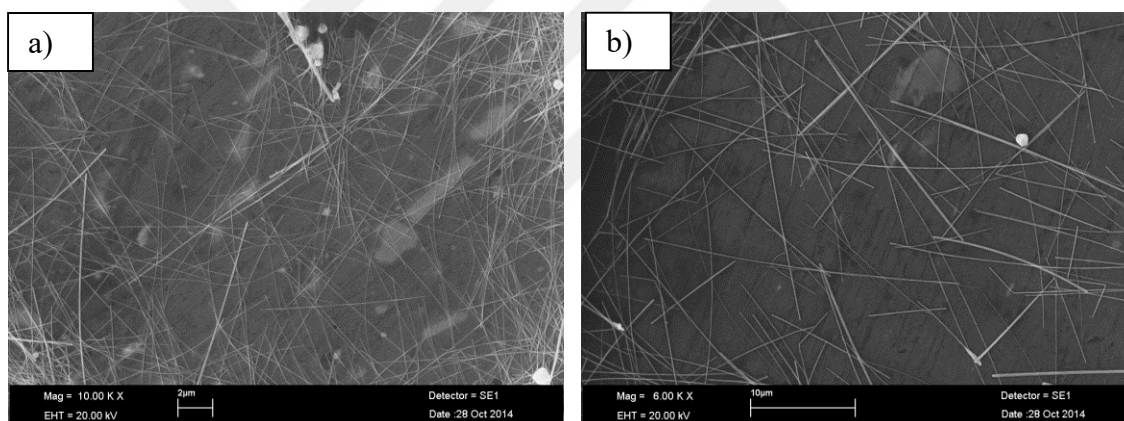
Figure 2.4.1.3 SEM images of silver nanowires with PVP360/AgNO$_3$ ratio of **a)** 1.5k, **b)** 2.5k.

Table 2.4.1.3 Length and diameter data of AgNWs synthesized with PVP360.

PVP/AgNO$_3$ molar ratio	Length (μm)	Diameter (nm)	L/D
0.5k	20	38	526
1.5k	30	58	517

*k=2.78x10^{-3}

In Figure 2.4.1.4, effect of the molecular weight of PVP polymer is clearly seen from the SEM images of silver nanowires synthesized by using different size PVP molecules.
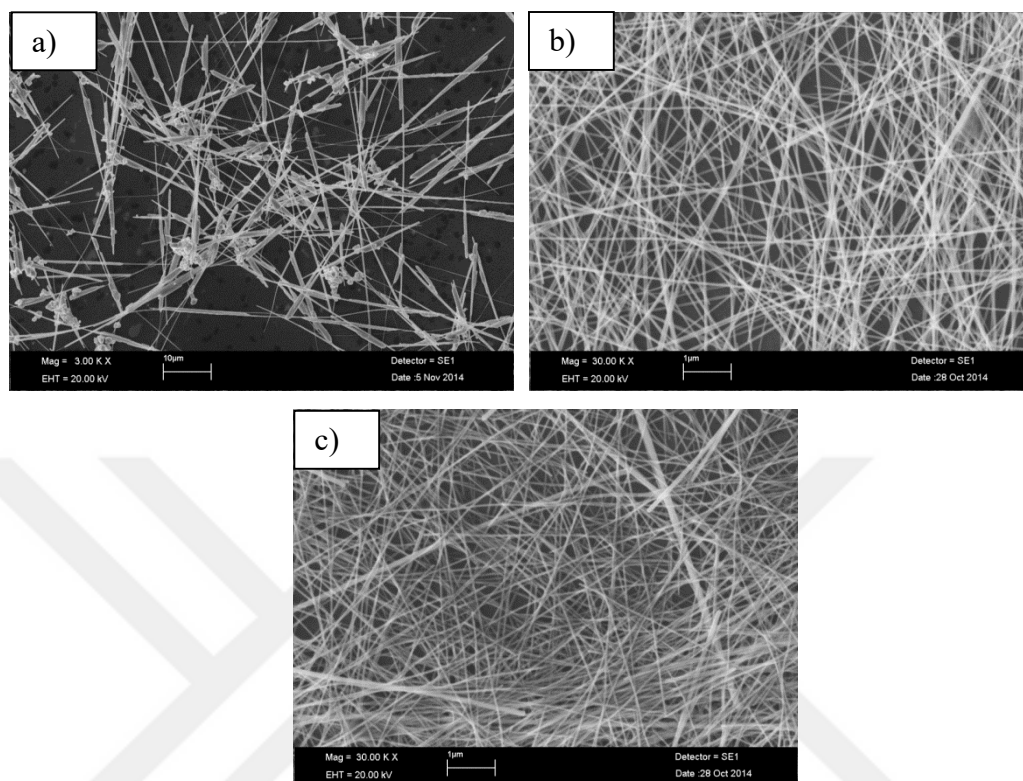
Figure 2.4.1.4 SEM images of silver nanowires with **a)** PVP10, **b)** PVP40 and **c)** PVP360.

According to the results from SEM, the best aspect ratio (L/D) was obtained (~600) when PVP40 was used as capping agent with a molar ratio of 3.5k between PVP and AgNO$_3$ although the longest nanowires were obtained in PVP10 when the molar ratio was 4.5k. But the length range is too high and the diameters are very big in the use of PVP10. The best aspect ratio in PVP10 use is half of the PVP40 case when the reaction duration is 45 min. After that point, length starts to decrease and nanowires are getting thicker. Besides, the reaction efficiency is very low for PVP10 used synthesis.

In the case of using PVP40, lengths of nanowires didn't show a significant difference when the molar ratio of PVP and AgNO$_3$ was 2.5k, 3.5k and 4.5k. But, there is a prominently decrease in diameter when this ratio is 3.5k.

Use of PVP360 can also provide very clear nanowire solution as in PVP40 use. In addition, lengths are longer when PVP360 is used, but diameters are also higher comparing to the case of PVP40, so the aspect ratio is lower. Reaction efficiencies for PVP40 and PVP360 are very good and the loss is low.

2.4.2. Coating of Silver Nanowire With Noble Metals

Galvanic exchange reactions were performed as described in the experimental section. Figure 2.4.2.1 shows the SEM images of Au coated silver nanowires with the precursor of $HAuCl_4$. It is clearly seen that the nanowires are still preserving their 1D shape after reaction. By this method, reduced gold nanoparticles accumulated on the surface of nanowires, but not making a smooth coating layer. With the increase in the amount of $HAuCl_4$, it was observed that the amount of nanoparticles on nanowire surfaces also increased.
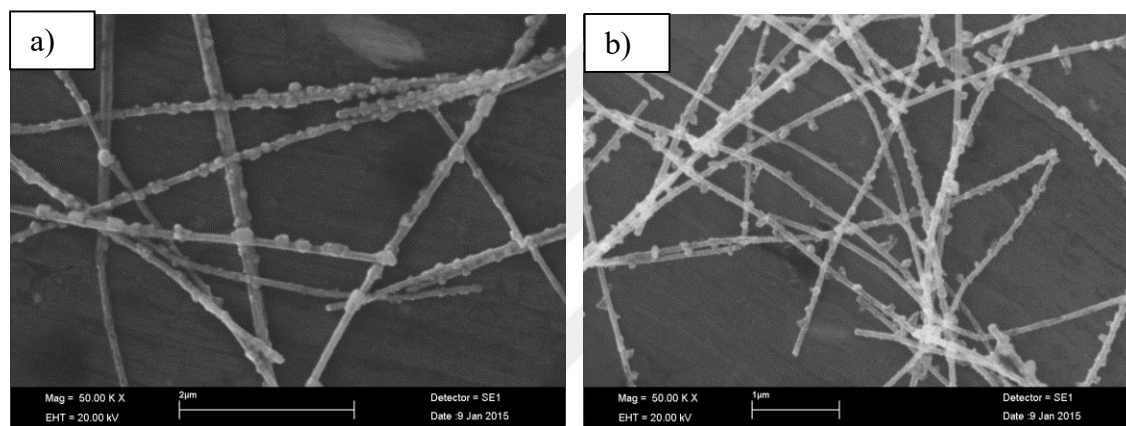
Figure 2.4.2.1 SEM images of Au coated silver nanowires with **a)** 8.11 ml, **b)** 13.52 ml of $HAuCl_4$

SEM image and UV-Vis absorption spectra of Pd coated silver nanowires was shown in Figure 2.4.2.2. For this experiment, $PdCl_2$ was used as palladium precursor. The products look very similar to ones coated with $HAuCl_4$. Palladium nanoparticles can be clearly seen on the nanowires. However, the linear shapes of silver nanowires were deformed probably because of the high amount of $PdCl_2$, and some bended and broken nanowire structures were obtained. These deformations can be prevented by optimizing the amount of Pd precursor.
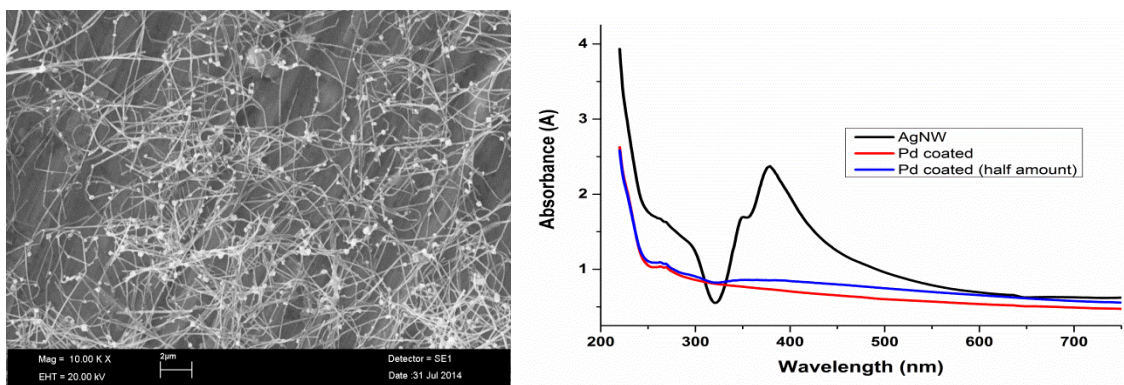
Figure 2.4.2.2 SEM image and UV-Vis spectra of Pd coated silver nanowires obtained by using $PdCl_2$ as Pd precursor.

For platinum coating, H_2Cl_6Pt was used. According to SEM image of the product of this experiment, shown in Figure 2.4.2.3, we can say that silver nanowire surfaces might be covered by Pt nanoparticles. But EDX results told us that the amount of Pt was quite high and it might not be only on the surface of nanowires, but also be infused inside the nanowires.
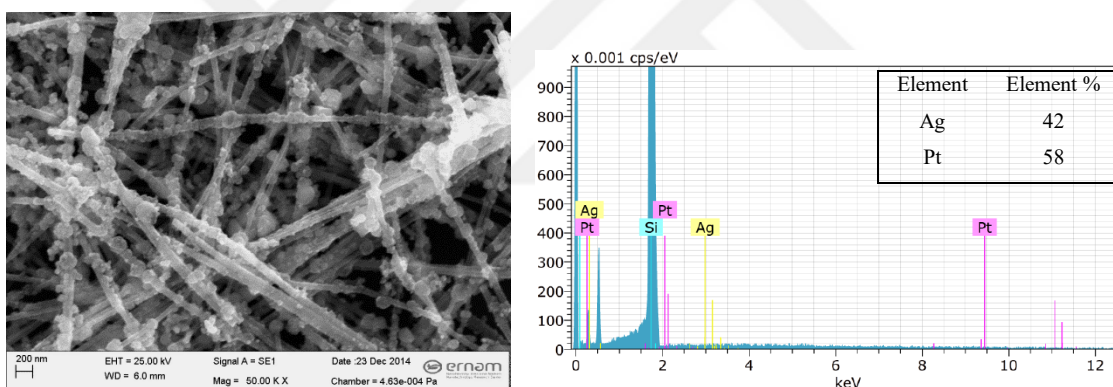
Figure 2.4.2.3 SEM image and UV-Vis spectra of Pt coated silver nanowires obtained by using H_2Cl_6Pt as Pt precursor.

The results of coating experiments with these three precursors showed us that it's not so possible to achieve a smooth noble metal layer on silver nanowire surfaces. In order to perform milder and more controllable galvanic exchange process, Kim et al. used $[Au(en)_2]Cl_3$ complex which has lower reduction potential than $HAuCl_4$ and they could obtain almost homogeneously Au coated surface for silver nanowires. In this study, we tried Pd and Pt complexes ($[Pd(en)_2]Cl_2$ and $[Pd(en)_2]Cl_2$) with the same approach. Figure 2.4.2.4 and Figure 2.4.2.5 show the SEM images and EDX results for Pd and Pt coatings with complex solutions via dropwise addition method. Findings showed us that the coating with these two complexes have been successful without a significant deformation on nanowire surfaces.
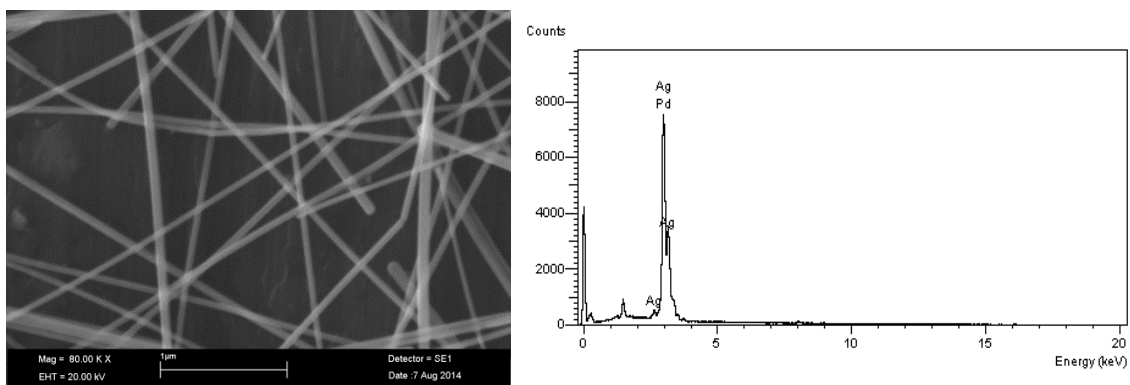
Figure 2.4.2.4 SEM image (left) and EDX result (right) of Pd coated AgNWs by using Pd complex ([Pd(en)$_2$]Cl$_2$).
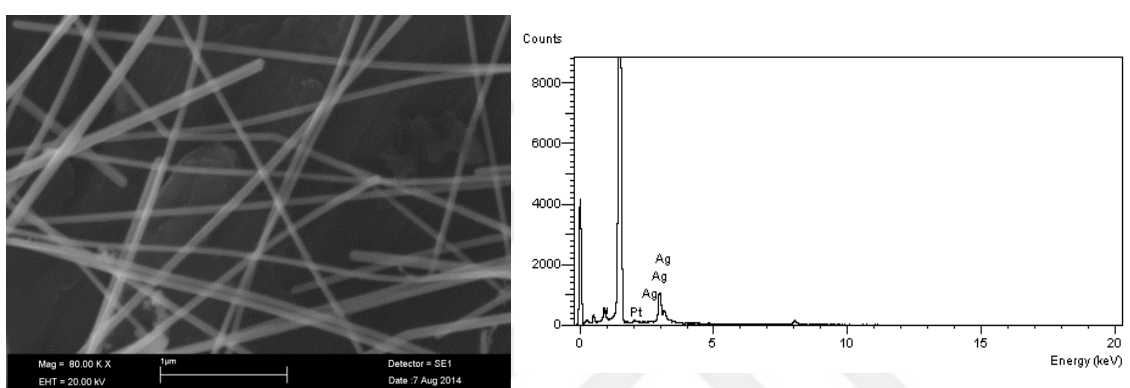
Figure 2.4.2.5 SEM image (left) and EDX result (right) of Pt coated AgNWs by using Pt complex ([Pt(en)$_2$]Cl$_2$).

When Pd and Pt complexes were used in biphasic titration method which was designed for slower and more controllable coating, almost the same coating ratio was achieved with Pd complex as it's seen in Figure 2.4.2.6. Coating process with Pt complex wasn't successful for this method.

Element	Element %
Ag	98.2
Pd	1.8
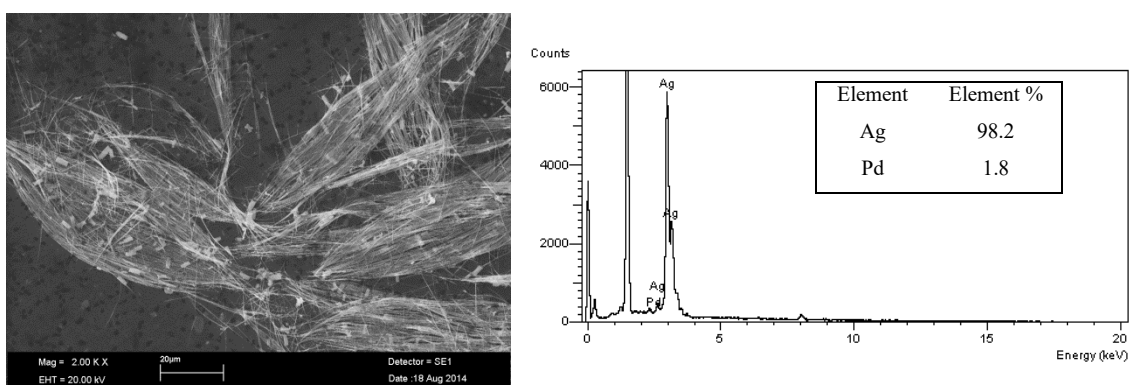
Figure 2.4.2.6 SEM image (left) and EDX result (right) of Pd coated AgNWs by Pd complex ([Pd(en)$_2$]Cl$_2$) via biphasic titration method.

2.5. Conclusion

This chapter involves the synthesis of silver nanowires by using different length polyvinylpyrrolidone (PVP) molecules. Among three PVP molecules (PVP10, PVP40, and PVP360), the best aspect ratio results were obtained when PVP40 was used as capping agent with 3.5k PVP/AgNO$_3$ molar ratio as 615. PVP10 remains too weak to prevent the growth on {100} facets, so the diameters range was found to be large. Also, the efficiency of nanowire formation was low.

For the passivation of the nanowire surfaces against oxidation, silver nanowires have already been coated with gold through galvanic exchange by Kim et al [35]. Our group published a study about Pd coating of silver nanowire by using different Pd complex ([Pd(en)$_2$](NO$_3$)$_2$) [47], but to the best of our knowledge, Pd and Pt complexes ([Pd(en)$_2$]Cl$_2$ and [Pt(en)$_2$]Cl$_2$) weren't studied before for silver nanowires. When tetrachloroauric acid (HAuCl$_4$), palladium (II) chloride (PdCl$_2$) and chloroplatinic acid (H$_2$Cl$_6$Pt) were used, nanowires were coated by individual nanoparticles on their surfaces rather than a smooth coated surface. Silver nanowires coated with Pd and Pt complexes showed better surface properties in terms of smoothness, which can be important for conductivity. However they still require further study for optimization, the results are promising for coating with complexes.

Chapter 3

Copper Nanowire

3.1. Literature Survey

3.1.1. Copper Nanowires as Transparent Conductors

Copper is another important alternative material to ITO due to its high conductivity, and relatively low cost compared to silver. These properties drove the researchers to study on copper nanowire (CuNW) based transparent electrodes.

Im et al. fabricated a transparent conductive electrode by using copper nanowire network by embedding nanowires on the surface of a transparent glass-fabric reinforced plastic film monolithically and they achieved a good optical and conducting performance as 82% T at 25 Ω sq^{-1} sheet resistance [48]. This method is also suitable to gain stability to nanowires against oxidation.

Coating nanowires on a polymer substrate is favorable than using a glass substrate in order to fabricate a flexible device. Using polymer substrate is also useful to gain the chemical resistance and stability to oxidation to metal nanowires when nanowire network is embedded partially into the substrate [7]. Cheng et. al. prepared two transparent electrode with copper nanowires, having average 80 nm of diameter and tens to hundreds micrometers of length, by using a glass substrate and an elastic poly(acrylate) matrix [7]. They reported that transparent electrode with embedded nanowires on the surface of polymer matrix showed better stability against oxidation after exposing air medium for certain periods. Furthermore, it was proved that using polymer substrate gains mechanical robustness in addition to flexibility to the electrode.

For the flexible and foldable CuNW electrode preparation, Yin et. al. performed vacuum filtration method [49]. After filtration of the copper nanowire solution by a filter paper (8 μm pore size), prepared film was sintered at high temperatures around 200 ºC for 1 h. The sheet resistance of the film didn't show a big difference even after 1000 bending test.

High aspect ratios with thinner and longer nanowires are important while studying with transparent conducting electrodes for reducing the sheet resistance and increasing transmittance. It also provides flexibility and stretching ability to device. Compared to silver nanowires, higher aspect ratios can be reached. Wu et al. presented a low cost transparent electrode consisted of high aspect ratio (up to 100000) copper nanofiber network formed by electrospinning [10]. These copper nanofibers showed high transmittance at low sheet resistance due to fused crossing points as 200 $\Omega.sq^{-1}$ at ~96% T, 50 $\Omega.sq^{-1}$ at ~90% T, and 12 $\Omega.sq^{-1}$ at ~80% T. In addition, synthesized Cu nanofibers also showed a good stability against oxidation with a slow increase in sheet resistance from 10 Ω to 18 Ω in 3 months under ambient conditions. They performed the synthesis of copper nanofibers in three steps: 1) Electrospinning of copper acetate-PVA solution onto a glass substrate, 2) Heating the polymer nanofibers at 500 ºC, in air for 2 h in order to get rid of the polymer components, 3) Reduction of CuO nanofibers into red Cu nanofibers by annealing under H_2 atmosphere at 300 ºC for 1 h [10].

3.1.2. Copper Nanowire Synthesis Methods

There are many studies for copper nanowire synthesis. Although these studies includes various methods such as electrodeposition, hydrothermal reduction, colloidal methods, and vapor-phase deposition [50], in general, self-assemble solution based synthesis methods are more favorable than the methods in which a template is used for nanowire growth.

Liu et al. developed a novel synthesis method for copper nanowires and nanorods [51]. This method basically depends on vapor generation and deposition of copper metal and growth as nanowire and nanorod shape on a substrate under vacuum conditions. After 1 h reaction, the product consisted on mainly nanorods, with diameters changing between 50-100 nm and length up to 20 μm, and less nanowires which have {111}

growth orientation. By this one-step method, the researchers brought a new aspect to template synthesis of metal nanowires.

Zhou et al. used a rod-like viruses as template for the synthesis of high dispersible 1D copper nanostructures with 40-45 nm in diameter and over 1 μm in length [52]. However, template synthesis methods have some disadvantages such as complicated multistep, defects in products and low reaction yields [51].

Solution based synthesis methods of copper nanowires can be classified into two main topics: the methods which alkylamines are used and which ethylenediamine (EDA) is used as directing agents [11].

Under the first topic, many different methods were developed which use different alkylamines such as octadecylamine (ODA) [53] and hexadecylamine (HDA) [48] as shaping agents.

Shi and coworkers achieved to synthesize single crystal ultra-long copper nanowires with 50-100 nm in diameter and length in several mm after a 48 h reaction period at 180 ºC in a Teflon-lined autoclave reactor by using ODA as a stabilizing agent to prevent the aggregation of copper nanoparticles in nucleation step and as a shape directing agent in the growth step [53]. For the same synthesis process, HDA was also used instead of ODA by Im et al. [48]. They obtained the average length and diameter values as 35 μm and 50 nm for nanowires, respectively after a 24 h reaction period at 120 ºC.

Copper nanowires can also be synthesized with another hydrothermal method which includes oleylamine and KBr as surfactants and ethylene glycol as reductant for Cu (I) ions. After two-step temperature process, the first step at 110 ºC for degassing and second step at 198 ºC for the rest of the reaction, single crystal, [110] direction grown copper nanowires with average 30 μm in length and 92 nm in diameter were obtained by Yin et al [49].

During the synthesis of copper nanowires, Cheng et al. used Pt nanoparticles in order to catalyze the growth. In this reaction, the precursor copper acetylacetonate [Cu(acac)$_2$] was added into the previously prepared and heated to 180 ºC liquid-crystalline medium by mixing HDA and cetyltrimethylammonium bromide (CTAB). After 12 h reaction period at 180 ºC, they could obtain copper nanowires with an average diameter and length as 80 nm and tens to hundreds of micrometers, respectively [7].

Under the second category, the main synthesis method was developed at 2005 by Zeng et al [54]. They proposed a reaction for the formation of 1D copper nanowires via the reduction of copper nitrate by hydrazine, in which EDA was used as capping agent. This method, which is carried out in a very basic medium, has quite low reaction temperature and requires shorter reaction time.

3.1.3. Coating Studies of Surface of CuNWs with Noble Metals

In the last years, many studies have been done for the modification of copper nanowire surface by replacing surface atoms with other materials in order to gain different properties to the nanowires. Mostly, copper nanowires were coated with palladium [55] and platinum [56-58] for the use as catalyst in methanol oxidation or hydrogen evolution reactions. Copper nanowires can also be modified as oxidation-proof by coating with noble materials as well as improving catalyst characteristics. With this purpose, we performed galvanic exchange reactions on copper nanowires with gold, platinum, and palladium precursors.

3.2. Experimental Section

3.2.1. Synthesis of Copper Nanowire with Hydrothermal Method

3.2.1.1. Materials

Copper (II) chloride ($CuCl_2$, 97%, Sigma-Aldrich) and Octadecylamine (ODA, ≥99.0% (GC), Sigma-Aldrich) were used in the synthesis of copper nanowires.

3.2.1.2. Synthesis Procedure

In this synthesis procedure, previously described hydrothermal synthesis method [53] was performed with some modifications. At the first step, 40 ml of $CuCl_2$ (12.5

mM) solution was prepared by dissolution of 0.5 mmol $CuCl_2$ into deionized water. Then, 1 mmol of octadecylamine (ODA) was added into the blue $CuCl_2$ solution and vigorously stirred overnight around 15 hours to obtain well dispersed suspension. The final solution then was transferred into a Teflon-lined autoclave of 50 ml capacity and placed into the oven for 2 days. In order to determine the temperature effect on the growth of copper nanowires, the experiment was repeated for different temperatures changing between 120-180 ^{o}C. After the reaction finished, the reactor was cooled down to the room temperature naturally. The product was removed from the reactor and nanowires were washed with n-hexane, deionized water, and ethanol for a few times and kept in hexane solution in order to prevent the oxidation.

3.2.2. Synthesis of Copper Nanowires with Solution Based Method

3.2.2.1. Materials

Copper (II) nitrate trihydrate ($Cu(NO_3)_2.3H_2O$, Merck), Ethylenediamine (EDA, $\geq$99.5% (GC), Fluka), hydrazinium hydrate ($N_2H_4.H_2O$, Merck), and sodium hydroxide (NaOH, 98-100.5%, Merck) were used in the synthesis of copper nanowires.

3.2.2.2. Synthesis Procedure

In a typical procedure of copper nanowire synthesis, an aqueous solution was prepared in a glass reactor by adding 0.05 mmol of copper nitrate into 10 ml of NaOH (15 M) solution. Then, 75.2 μl of EDA and 6.8 μl of hydrazine were added into the just prepared solution, respectively, and the reactor was capped and shaken for a few minutes after addition of each component in order to disperse them homogenously (molar ratio; 1:3000:22.5:2.8 for $Cu(NO_3)_2$:NaOH:EDA:N_2H_4). After preparation of this final solution, the reactor was placed in an oil bath adjusted to varied temperatures between 40-90 C^{o} to understand the effect the temperature on copper nanowire formation. The blue color of the solution disappeared in a couple of minutes and became clear. In 10 minutes after the color vanished, formation of copper nanowires was observed by the color change into red. Because of the high density of the solution

and the bubbling as a result of N_2 formation, the product started accumulating on the top and a reddish fluffy texture was formed above the solution. After reaction completed and color of the solution under the nanowires turned clear, the glass reactor removed from the oil bath and was cooled down in an ice bath. Synthesized copper nanowires were washed with DI-H_2O first until the pH of solution became neutral. Then the product washed with methanol and stored in it or dried in a vacuum oven after washing with methanol and stored in a desiccator to prevent oxidation.

3.2.3. Coating of Copper Nanowires with Noble Metals

Different methods were tried to be applied to coat the surface of copper nanowires with noble metals such as Au, Pd, and Pt.

Au coating on copper nanowires was performed by using $HAuCl_4$ as gold precursor through following process. 7.64 ml of 0.25 mM $HAuCl_4$ was added into 20 ml of diluted CuNW solution, which was prepared by addition of 19 ml methanol into 1 ml CuNW solution (1.3 mg/ml), at 65 ^{o}C. 30 min after $HAuCl_4$ addition, reaction was finished and final solution was cooled down to the room temperature and washed with methanol.

For Pt coating on copper nanowires, H_2Cl_6Pt was used as Pd precursor as explained in following process. 2 ml of CuNW solution (1.3 mg/ml) was diluted to 15 ml by methanol and the diluted solution was heated up to 65 ^{o}C in an oil bath. Then 3.6 ml H_2Cl_6Pt solution (1 mM) was added drop by drop while stirring. After addition of Pt solution, the solution was left to cool down and then the product washed with methanol a few times by using centrifugation. The final product was stored in methanol.

Au, Pd, and Pt coatings were also performed by using complex solutions of these metals ($[Au(en)_2]Cl_3$, $[Pd(en)_2]Cl_2$, $[Pt(en)_2]Cl_2$) to achieve milder reaction rates. These noble metal complexes were used to coat CuNW surface by using two different methods: direct addition drop by drop and biphasic coating.

In direct addition method, 9.5 ml hegzan was added into 0.5 ml of CuNW solution (5 mg/ml). Then 5.1 ml complex solution (0.25 mM) was added drop by drop while stirring. After addition of complex, the solution was stirred for 2 h.

In biphasic method, 9.5 ml hegzan was added into 0.5 ml of CuNW solution (5 mg/ml). In another flask, 1 ml of complex solution was prepared by diluting 1 ml 9.25

mM of complex with 2 ml of water. Then this freshly prepared complex solution was added slowly. The same washing process was applied and the product was stored in methanol. This method as also performed with $HAuCl_4$, too.

3.3. Characterization

3.3.1. Scanning Electron Microscopy (SEM)

Surface morphology and size of nanowires were determined by ZEISS EVO LS10 scanning electron microscopy (SEM) and transmission electron microscopy (TEM).

3.3.2. Energy Dispersive X-Ray Spectroscopy (EDX)

Bruker energy dispersive X-ray spectroscopy (EDX) was used to understand the composition of copper nanowires.

3.3.3. X-Ray Diffraction

Crystallographic properties of copper nanowires were analyzed by Bruker Advance D8 X-ray diffractometer (Cu source with λ=1.5406 Å).

3.4. Result and Discussion

3.4.1. Characterization of Copper Nanowires Obtained by Hydrothermal Method

In hydrothermal synthesis method, copper (II) ions, which appeared in the solution as a result of the dissolution of $CuCl_2$ in water, were reduced into metallic copper by octadecylamine (ODA) under hydrothermal conditions. As a result of a successful reaction, the blue color of the suspension disappears and reddish fluffy textured product, which indicates the metallic copper nanowires formation, is obtained.

This reduction mechanism is a highly temperature depended process. With the intent of investigating the effect of temperature on this reaction, the process was carried out under different temperatures in a range of 120-180 ºC while other parameters were kept constant and the results were shown in Table 3.4.1.1.

In the literature, nanowire formation could be observed at low temperatures such as 120 ºC. Although the nanowires had more uniform diameters at lower temperatures, crystallinity of the nanowires improved with the increase in temperature [53].

In this study, we couldn't observe nanowire formation at lower temperatures than 160 ºC. In Figure 3.4.1.1, a few copper nanowires are seen from the SEM images. The generated nanowires didn't have homogeneous shape and uniform diameters.

There are also other copper nanostructures such as nanorods in addition to nanowires. Besides, a large number of cubic nanoparticles were observed in Figure 3.4.1.1. Separation process of copper nanowires from the rest of the solution is difficult and the reaction yield is too low. When the reaction period increased, it was observed that the reaction yield also increased.
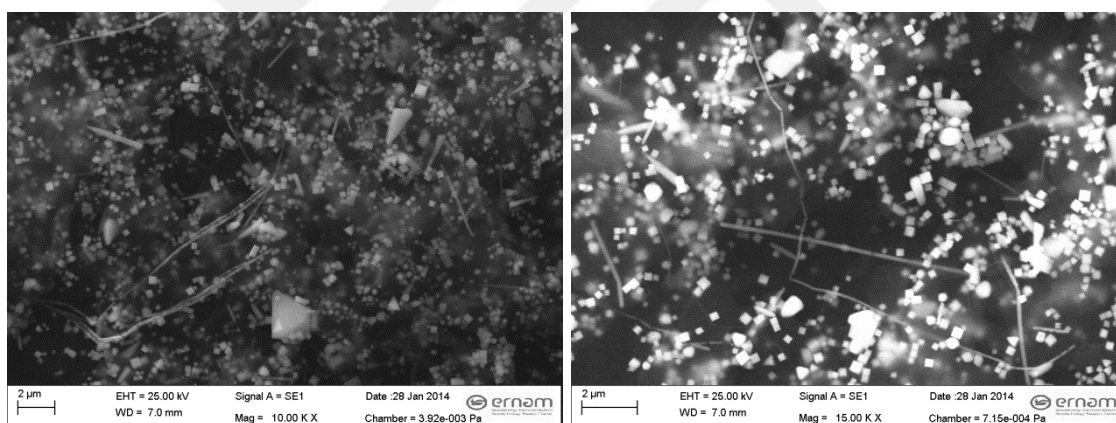
Figure 3.4.1.1 SEM image of the product synthesized at 160 ºC for 48 h.

Table 3.4.1.1 Information about copper nanowire formation at different temperatures for hydrothermal synthesis method.

Reaction period	Temperature (ºC)	Result
48 h	120	No CuNW formation
48 h	135	No CuNW formation
48 h	140	No CuNW formation
48 h	150	No CuNW formation
48 h	160	Low yield CuNW formation
48 h	165	Low yield CuNW formation
48 h	180	High yield CuNW formation
84 h	165	CuNW formation

When the reaction is performed at 185 °C, it was clearly seen that the yield of the copper nanowire formation enhanced significantly. The resulting solution after reaction finished looked like consisting of two separated layers. Upper part of the solution is shown in Figure 3.4.1.3. Since big part of the copper nanowires gathered at the bottom layer, CuNWs were separated easily by washing with n-hexane, deionized water, and ethanol. Figure 3.4.1.2 shows the final nanowire product kept in hexane and its SEM images. Obtained nanowires were 90-120 μm in length and 20-500 nm in diameter. As it is seen in Figure 3.4.1.2, the synthesized nanowires at 185 °C have varying diameters in a wide range.

During the formation of copper nanowires by hydrothermal process, ODA has a ligand-assisted template role in addition to its reductive property [53]. So, there is no need to use another surfactants or reducing agent to synthesize nanowires in this method.

Aliphatic amines such as ODA form micelles in aqueous medium and the lone pair electrons on the nitrogen atom gains nucleophilic character to ODA. This nucleophilicity induces ODA molecules to surround Cu^{2+} cations and keep them in an interphase. By the increasing temperature, ODA molecules are rearranged to form lamellar phase structures and these structures work as micro reactors for the formation of nanowires [53].
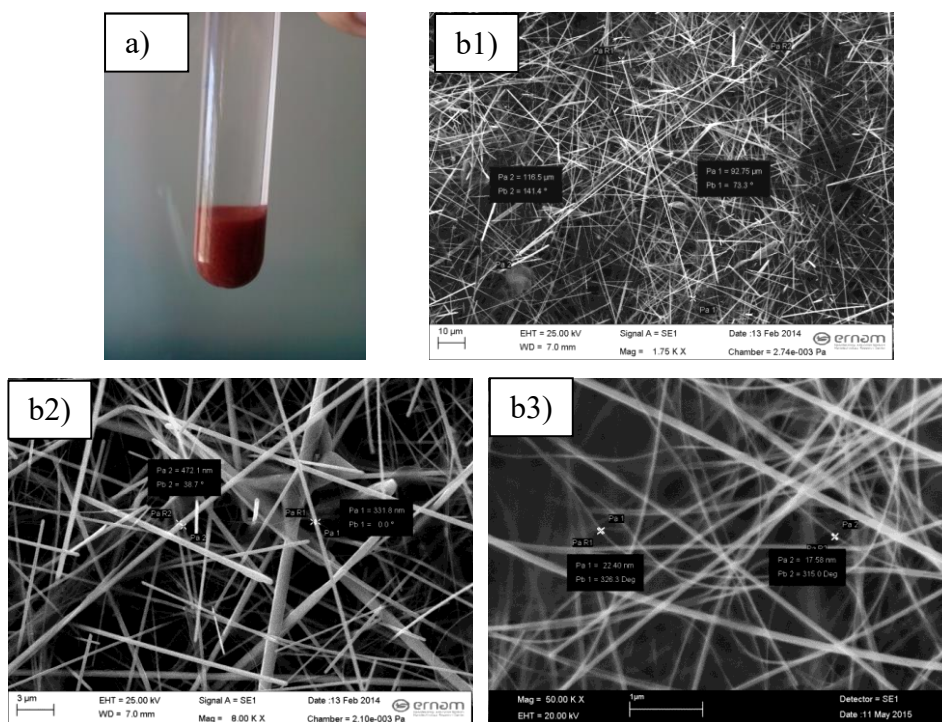
Figure 3.4.1.2 a) Photos and **b)** SEM images of the copper nanowires extracted from the bottom layer of the resulting solution after the reaction at 185 °C, after 48 h.
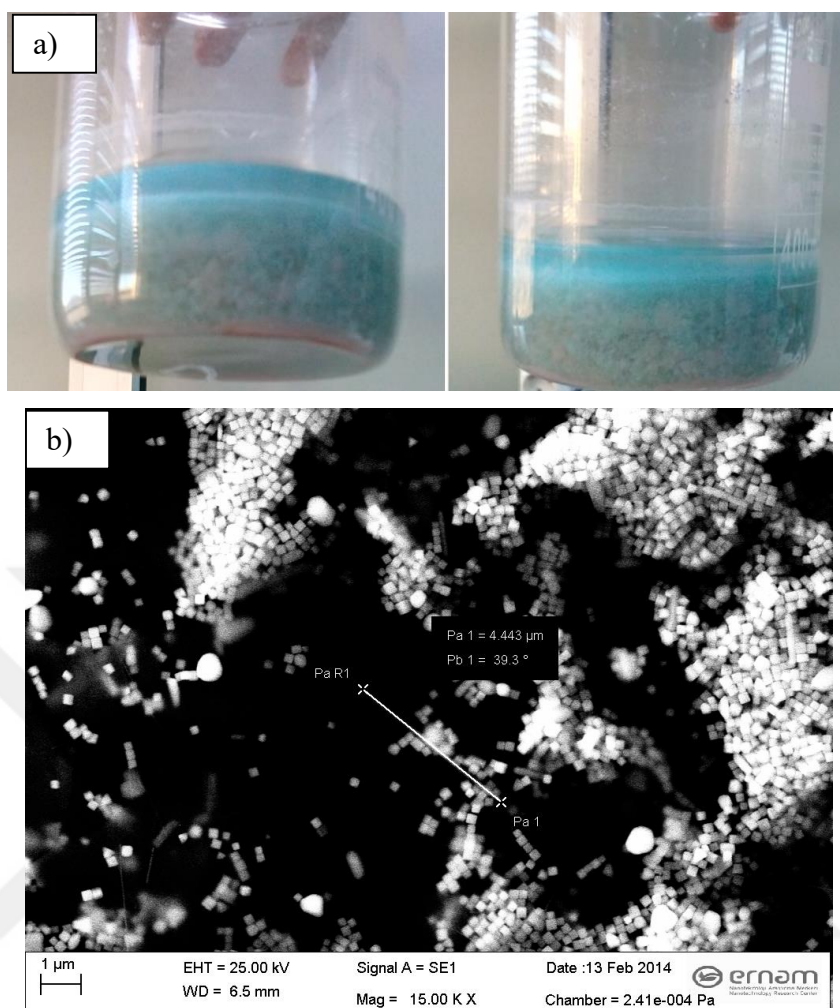
Figure 3.4.1.3 a) Photos and **b)** SEM images of upper layer of the resulting solution after the reaction at 185 ºC, after 48 h.

3.4.2. Characterization of Copper Nanowires Obtained by Solution Based Method

Ethylenediamine was used as shape directing agent to force the growth of copper in one direction to get nanowire shaped structures. Copper (II) ions were reduced by hydrazine in a very basic medium (15 M). In an attempt to examine the temperature effect on the growth, the reaction was repeated at different temperatures varying between 40-90 ºC. Figure 3.4.2.1 and Figure 3.4.2.2 show SEM images of copper nanowires synthesized at different temperatures and size measurements are given in Table 3.4.2.1.

As it is clearly seen in the Table 3.4.2.1, temperature change has a great effect on nanowire size, especially on diameter. When the reaction was performed at 90 ºC,

diameters of nanowires increased significantly while the length decreased. Although the best aspect ratio (L/D) result was obtained from the nanowires synthesized at 40 ºC, average diameter of nanowires are quite big. Furthermore, homogeneity of nanowires is not good at this temperature. Most of the nanowires looked like formed by the sequentially attached big particles. The best result was obtained at 70 ºC in terms of homogeneity along the nanowires and size.

The nanowires obtained with this synthesis method shows a different characteristic compared to the previous hydrothermal method. There are spherical nanoparticles attached to the one edge of the nanowires as it is clearly seen in Figure 3.4.2.1 and Figure 3.4.2.2. Rathmell and coworkers [59] had performed an experiment to determine if these edge particles were the starting point of nanowire growth or they formed after the 1D growth. For this investigation, they stopped the reaction after different times and examined the products with electron microscopy. The results showed that nanowire growth starts from these spherical particles

Table 3.4.2.1 Length and diameter measurements of CuNWs synthesized at different temperatures.

T (ºC)	40	50	60	70	80	90
Av. Diameter (nm)	110	85	150	95	105	215
Av. Length (µm)	60	25	40	25	25	12
L/D	545	294	267	263	238	56

Crystallographic properties and purity of nanowires, synthesized by using EDA as shape directing agent, were analyzed by using XRD method and the results were shown in Figure 3.4.2.3. Three peaks at $2\theta=43.3^\circ$, 50.4° and 74.2° respectively correspond to the {111}, {200} and {220} planes of a single crystalline fcc copper [9]. There is not any other diffraction peak showing the existence of impurities such as CuO or Cu_2O for the as prepared samples. So as to understand the oxidation resistance of copper nanowires, samples were stored for 4 months in a desiccator at room temperature. Figure 3.4.2.3 also indicates that copper nanowires have very high stability against oxidation even after 4 months under room conditions.
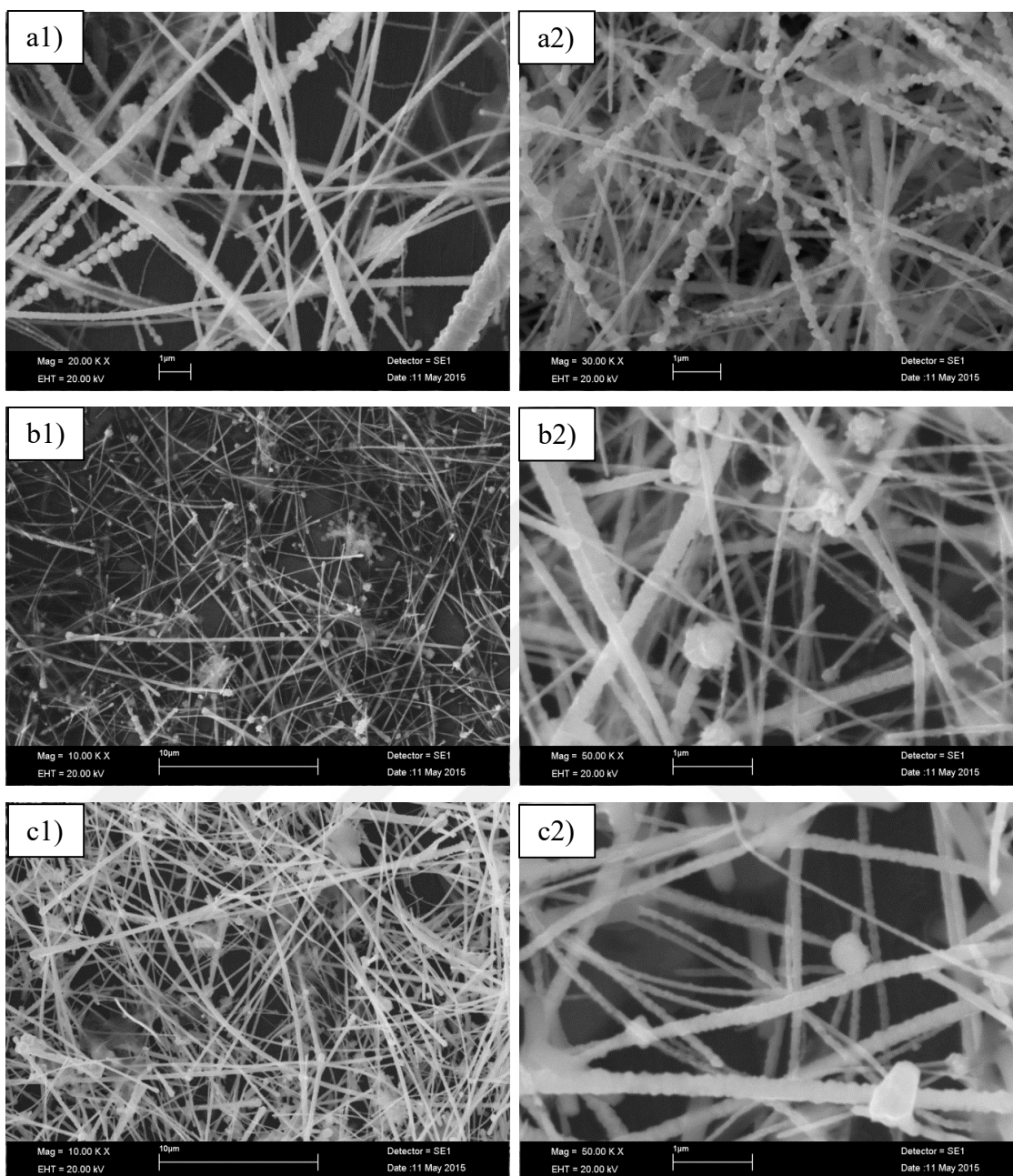
Figure 3.4.2.1 SEM images of copper nanowires synthesized at **a)** 40 ºC, **b)** 50 ºC, and **c)** 60 ºC.
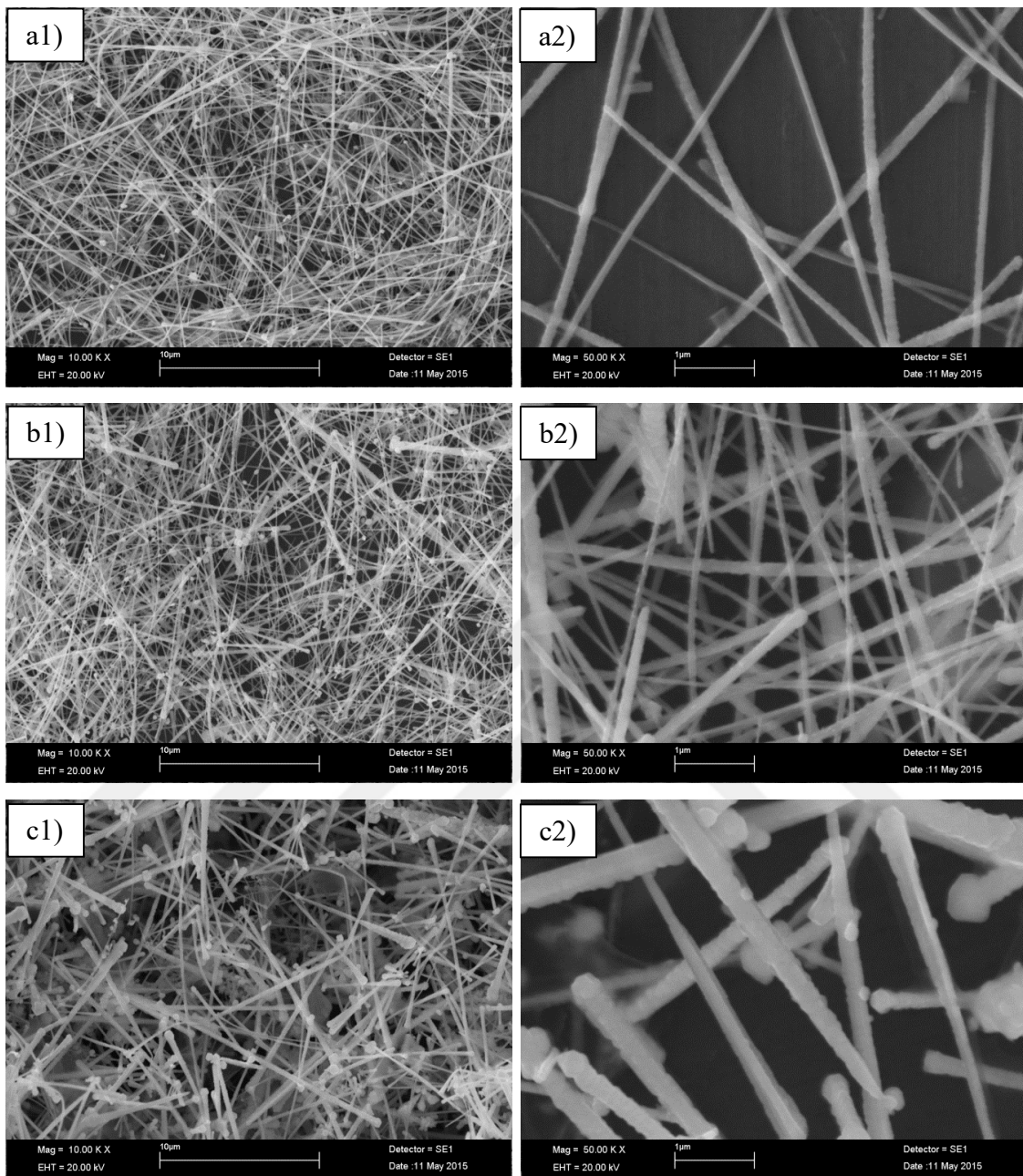
Figure 3.4.2.2 SEM images of copper nanowires synthesized at **a)** 70 ºC, **b)** 80 ºC, and **c)** 90 ºC.
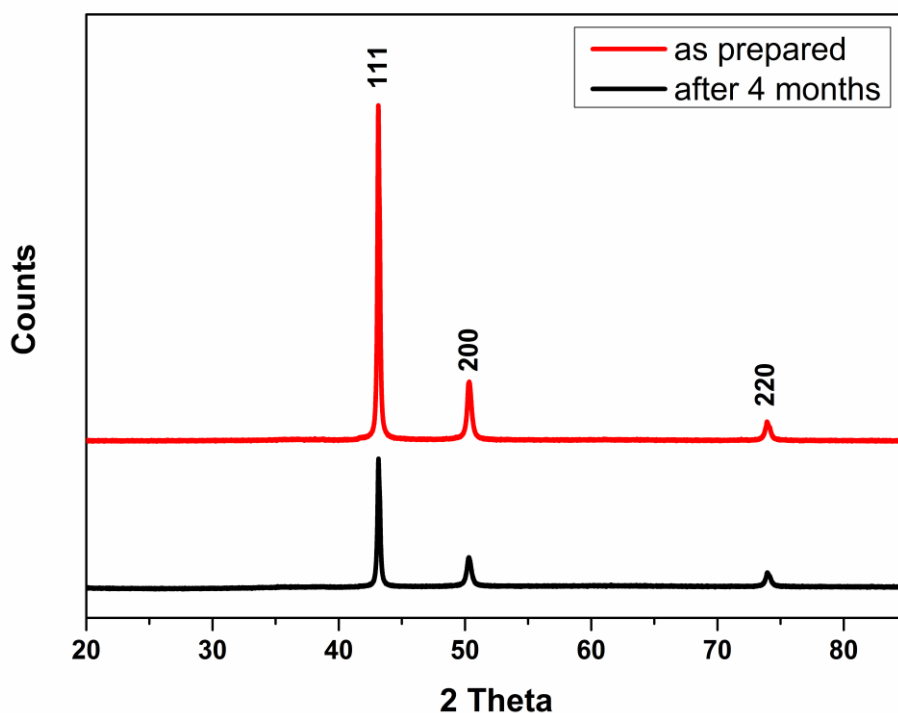
Figure 3.4.2.3 XRD patterns of copper nanowires **a)** as synthesized; **b)** kept for 4 months.

The shape of nanomaterial is directly depended on surface energy gap [49], and by using some surfactant molecules these energies can be altered to have different nanomaterials with different structures. The plane energies of copper is {110}>{100}>{111} [9] as an fcc material.

Reduction mechanism of copper (II) ions into metallic copper in the alkaline condition by hydrazine was shown in the following reaction:

$$2Cu^{2+} + N_2H_4 + 4OH^- \rightarrow 2Cu + N_2 + 4H_2O \qquad (3.4.2.1)$$
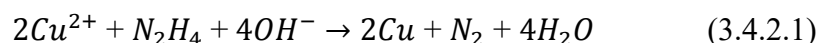
Through the reaction, the blue color disappeared completely and red color formed, which indicates the total conversion of Cu^{2+} ions into metallic copper.

Comparing to the other synthesis methods for CuNWs, this method requires less temperature (70 °C) and reaction period (~15 min). Also it is convenient for large-scale production. Although the reaction requires longer time with the increase of material amount for larger scale production, this method is still the one who has the shortest reaction period comparing to the other synthesis methods for the same scale production. Furthermore, synthesized copper nanowires can easily disperse in methanol by shaking.

In this synthesis, EDA has an important role as a shape directing agent for the anisotropic growth of CuNWs. EDA molecules have the ability to adhere on {100}

46

plane of fcc copper nanoparticles and prevent the growth on this surface, so the elongation occurs along the {110} plane [54] of copper which has higher energy than {111} [49]. In the absence of EDA, only nanoparticles tend to be formed [11,59].

Rathmell et al. performed the reaction for different EDA quantities in order to investigate the preferential attachment of EDA molecules to the copper facets [59]. Up to some concentration, the diameters of nanowires were decreasing while the lengths were increasing. But after some point, increase in EDA concentration resulted in an increase in diameter and a decrease in length because the high concentration of EDA molecules capped the ends besides the sides of copper.

3.4.3. Coating of Copper Nanowire With Noble Metals

Galvanic exchange reactions were performed as described in the experimental section. In Figure 3.4.3.1, the SEM images of Au coated copper nanowires with the precursor of $HAuCl_4$ were presented with EDX results. Due to the excessive amount of gold precursor, copper nanowires were broken into smaller pieces. Also a significant increase was observed in the thickness of nanowires.
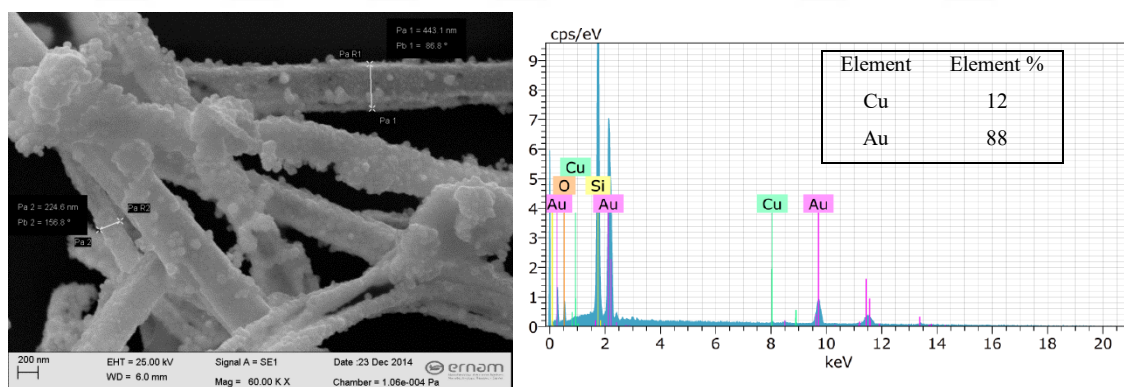
Figure 3.4.3.1 SEM image and EDX result of Au coated CuNWs obtained by using $HAuCl_4$ as Au precursor.

H_2Cl_6Pt was used for platinum coating and better results were obtained compared to previous gold coating experiment. According to SEM image of the product, showed in Figure 3.4.3.2, smoother coating could be achieved. However, it is still too much Pt on nanowires as it's clearly seen in EDX results and nanowires were broken into smaller pieces, too.
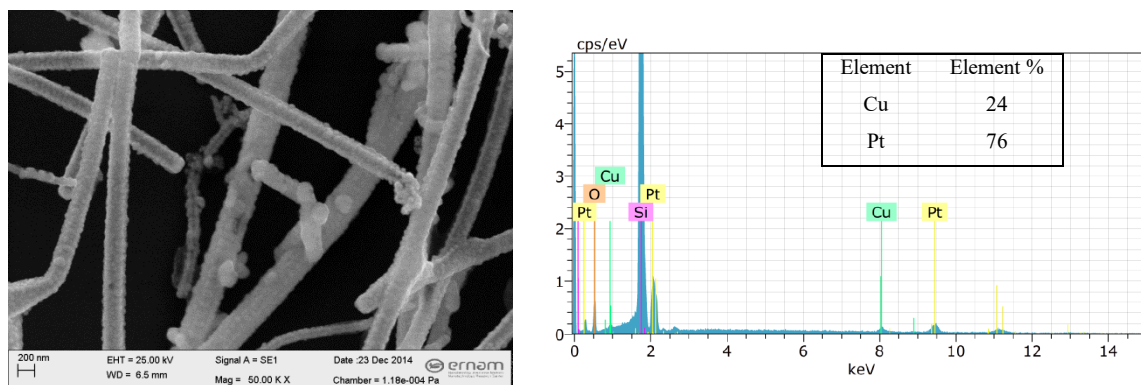
Figure 3.4.3.2 SEM image and EDX result of Pt coated CuNWs obtained by using H_2Cl_4Pt as Pt precursor.

In order to provide milder reaction conditions, complex solutions of Au, Pd, and Pt was used for coating of the copper nanowires, too. For the dropwise addition method, none of the complex solutions worked and any coating value couldn't be achieved. In the biphasic method, Pd complex wasn't successful again, but copper nanowires could be coated with Au and Pt by using complex form of these metals ($[Au(en)_2]Cl_3$ and $[Pt(en)_2]Cl_2$) in addition to $HAuCl_4$ and the results showed in Figure 3.4.3.3, 3.4.3.4, and 3.4.3.5. Some structural deformations of nanowires, such as bended and broken parts, were observed for the cases gold and platinum complexes were used. On the other hand, $HAuCl_4$ showed better results in terms of preserving the nanowire structure. Also the gold nanoparticles can be clearly seen on the nanowire surface.

Figure 3.4.3.3 SEM image and EDX result of Au coated CuNWs obtained by using $HAuCl_4$ as Au precursor through biphasic method.

48
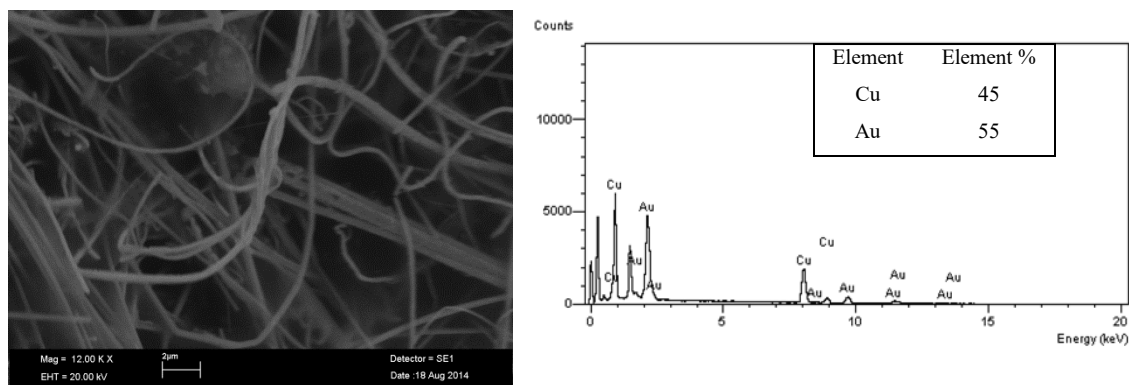
Figure 3.4.3.4 SEM image and EDX result of Au coated CuNWs obtained by using Au complex [[Au(en)₂]Cl₃] as Au precursor through biphasic method.

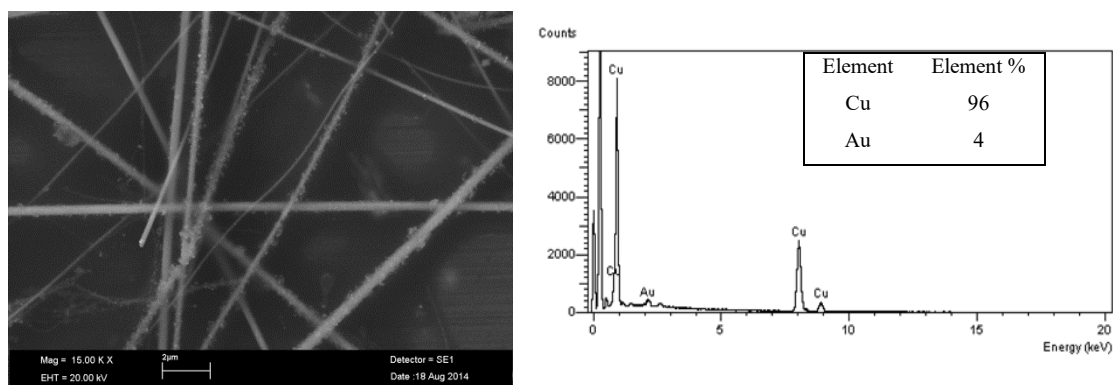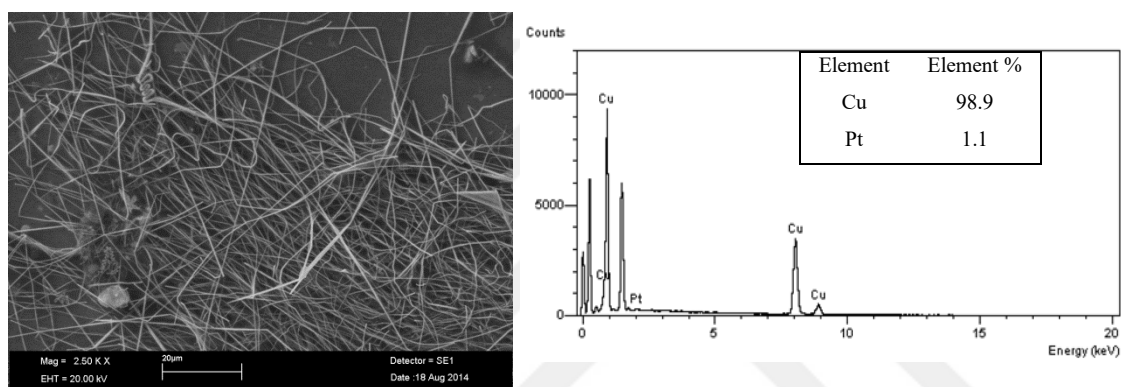**Figure 3.4.3.5** SEM image and EDX result of Pt coated CuNWs obtained by using Pt complex [[Pt(en)₂]Cl₂] as Pt precursor through biphasic method.

3.5. Conclusion

This chapter reports the synthesis of copper nanowires with two different methods and the coating studies of nanowire surfaces through galvanic exchange process by using different noble metal precursors.

In the synthesis part, temperature for the hydrothermal method optimized as 180 ºC in order to obtain very long (90-120 μm) copper nanowires with 20-500 nm in diameter. Although the aspect ratio of these nanowires is quite high, which is desirable for display applications, low dispersibility of the product is still an obstacle for appropriate coating of a substrate with these nanowires. Solution based method requires lower reaction temperature (optimized as 70 ºC) and shorter synthesis period (around 30 min) compared to hydrothermal process. In addition, the product showed very good dispersibility in methanol and water. XRD results confirmed that these copper

nanowires also have a good stability against oxidation under room temperature and atmosphere even after 4 months.

Galvanic exchange studies were performed for the copper nanowires synthesized by hydrothermal method by using different Au, Pd and Pt metal precursors. Dropwise addition of $HAuCl_4$ and H_2Cl_6Pt caused harsh redox reactions between these precursors and CuNWs and ended up with fractures of nanowires. According to the EDX results of nanowires, which are products of dropwise addition coating by using Au, Pd and Pt complexes, there isn't any inert metal on CuNWs, so this method failed for complex solutions. In the biphasic coating method, promising results were obtained by using $HAuCl_4$, Au and Pt complexes. But further studies are still required to optimize the coating methods.

Chapter 4

Catalytic Application of Copper Nanowires

4.1. Literature Survey

4.1.1. Nanomaterials For Catalytic Applications

Nanomaterials which have various shapes have been studied for the degradation of organic dyes. Some of these nanomaterials can have rod shape while some are spherical, cubic and so on. In Figure 4.1.1.1 there are two different examples of catalysts with different structure. First one is belt-like TiO_2 photocatalyst (50–200 nm in width, 20-40 nm in thickness). It has found that hydrogenated TiO_2 shows catalytic activity on the methyl orange degradation [60]. Second is tetrabutyl ammonium bromide stabilized Co NPs, which are around 90 nm in diameter, were studied for degradation of methylene blue (MB), methyl orange (MO) and rhodamine B (Rh-B) by using $NaBH_4$ as a reducing agent [61,62].
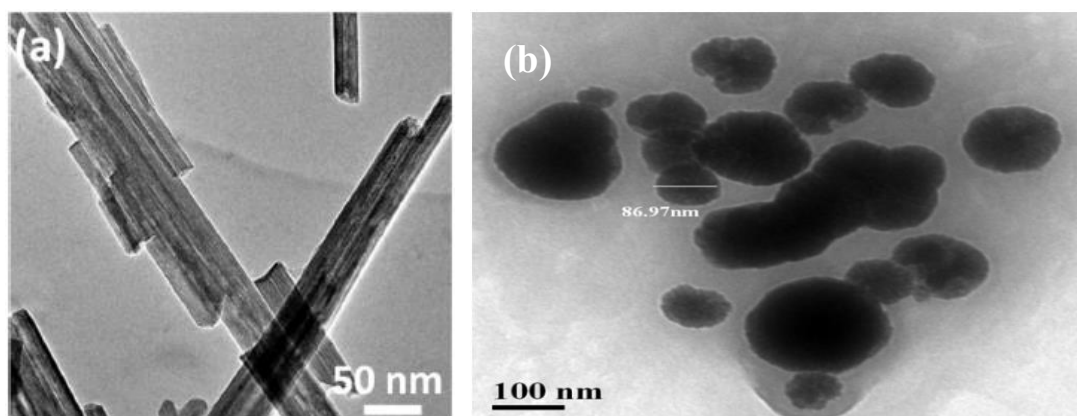
Figure 4.1.1.1 Different catalyst structures studied for the degradation of dyes **a)** Belt-like TiO_2 photocatalyst **b)** Co NPs, around 90 nm in diameter.

Palladium structures are one of the most studied catalysts for the catalytic oxidation of methylene blue [63]. TiO_2 photocatalyst [60], gold [64], silver [64-66], and platinum nanoparticles [64] are other studied catalysts for dye degradation. In Figure 4.1.1.2, UV-Vis absorption graphs of catalyzed and uncatalyzed MO degradation reactions are shown. The catalytic effects of Ag, Au, and Pt nanoparticles on the reaction rate are clearly seen. Although these materials show catalytic effect on the dye degradation reactions, they are generally expensive and rare materials. This makes them unfeasible for large scale reactions.
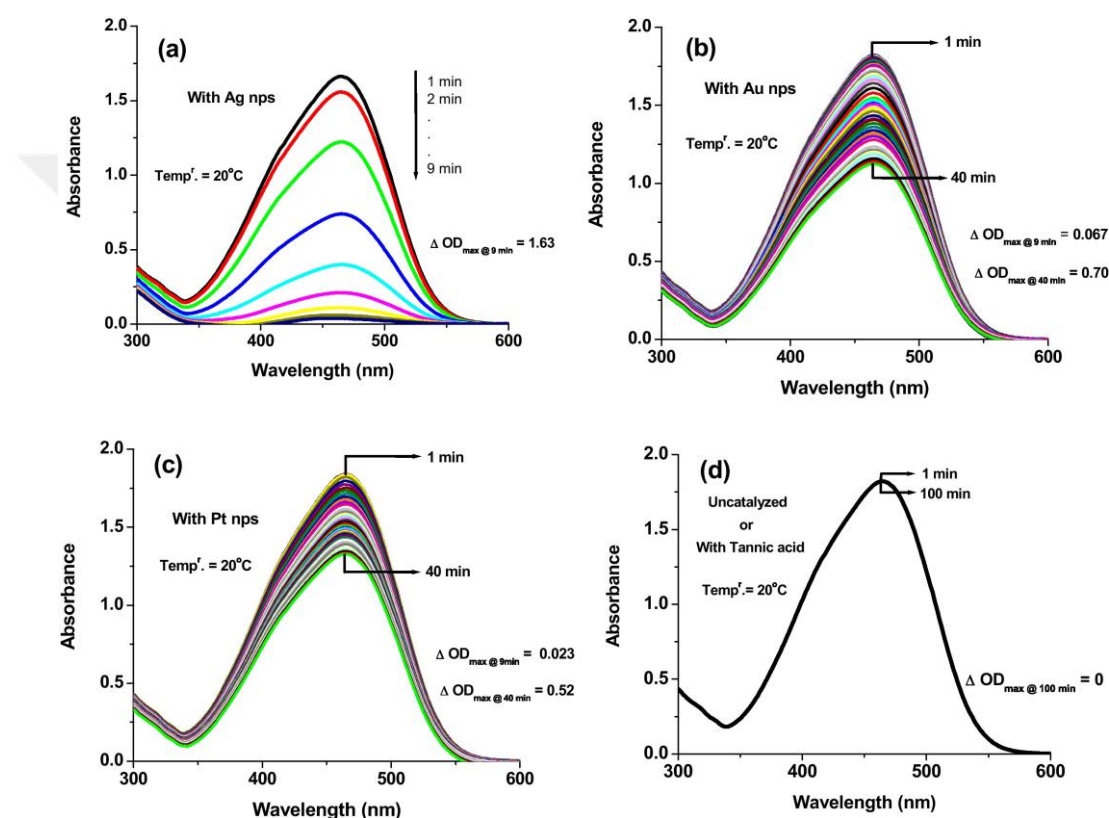
Figure 4.1.1.2 Comparison of plot of absorbance versus wavelength for the reduction of methyl orange in the presence of $NaBH_4$ at 20 ºC using **a)** Ag NPs, **b)** Au NPs, **c)** Pt NPs whose diameters are around 10 nm, and **d)** only tannic acid (uncatalyzed) [64].

Copper is also known to show some catalytic properties. Catalysts have a very important role in reactions to lower the required energy, reduce the time for reaction, and increase product yield. Copper nanostructures are also used as catalyst applications. For catalytic applications, mostly nanoparticle form of copper is used [67].

For the degradation of methylene blue, methyl orange, and rhodamine B, catalytic activity of cobalt nanoparticles had also been reported [61,62]. Copper particles [68] were also tested for their catalytic performance on these degradation reactions. Wang et al. synthesized hollow copper microspheres as catalyst [69,70]. Other copper catalysts

such copper based metal organic frameworks [71] were also reported for dye degradation.

There are some catalysis applications in which nanowires had been used as well. Zhang et al. investigated Pd deposited silicon nanowires on the degradation of methylene blue [72] and Au decorated selenium nanowires [73] was reported as catalyst for these reactions. In addition to the high cost of this kind of catalysts arising from Au and Pd, the synthesis also requires more than 1 step and difficult stages.
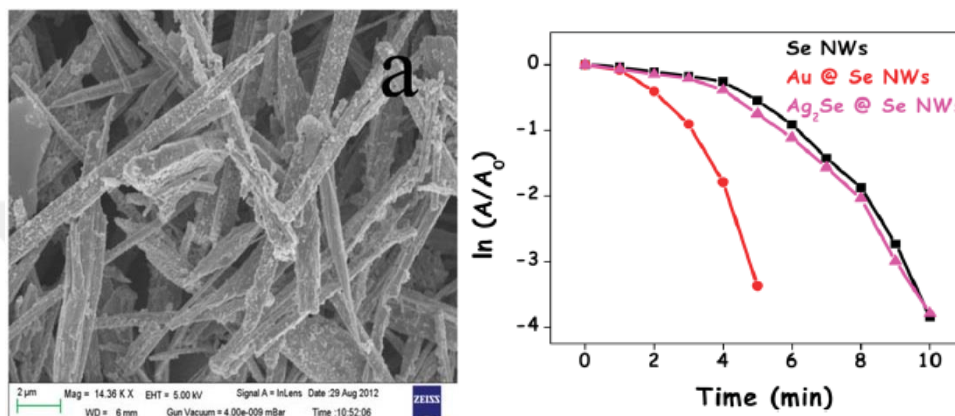
Figure 4.1.1.3 FESEM image of Au (0) deposited Se NWs and catalytic performance of different Se catalysts [73]

Various application fields have already been presented for copper in nanowire form. It has been showed that CuNWs can be used as transparent conducting electrodes (TCEs) [48,49,74], thermal interface materials [75], and proton exchange membrane fuel cells (PEMFCs) [76]. In this study, we investigate the catalytic performance of copper nanowires for an environmental problem. The reason of choosing copper nanowires as catalysts is abundancy, low cost and catalytic properties of copper basically. CuNWs showed very good catalytic performance on the degradation reactions of MB, MO and Rh-B.

4.2. Experimental Section

4.2.1. Materials

Copper (II) chloride ($CuCl_2$, 97%, Sigma-Aldrich) and Octadecylamine (ODA, ≥99.0% (GC), Sigma-Aldrich) were used in the synthesis of copper nanowires.

4.2.2. Catalytic Degradation Process

Catalytic activity of CuNWs was investigated by performing degradation processes of three organic dyes called methylene blue, rhodamine B and methyl orange, with the presence of $NaBH_4$.

In a typical test for methylene blue degradation, 5 ml of freshly prepared $NaBH_4$ solution (0.04 M) and changing amount of catalyst solution with 0.2 mg/ml concentration, which was prepared by dispersing dried copper nanowires in deionized water, were added into 15 ml of MB solution (1.87×10^{-4} M) and mixed. Then 3.5 ml of final solution was transferred to a quartz cuvette immediately and the cuvette was capped. Absorption spectra during the catalytic degradation were recorded by UV-Vis spectrophotometer versus time until MB was completely degraded at ambient conditions. For the catalytic reaction of methyl orange, the procedure is the same with MB reaction. In the catalytic reaction test for rhodamine B, 5 ml of 0.02 M $NaBH_4$ solution and 15 ml of 3.33×10^{-5} M Rh-B solution were used instead of the concentration in other two dyes. The procedure is also the same for Rh-B.

4.3. Characterization

UV-Vis spectra for following the catalytic degradation reactions were obtained from Shimadzu UV-1800 spectrophotometer.

4.4. Result and Discussion

Organic dyes (MB, Rh-B, and MO) were used to examine the catalytic performance of copper nanowires. One of the reasons we chose these three dyes is simply that they show strong colors, which are observable with human eye and the change in colors as a result of degradation reactions, makes easy to follow the process. In addition, they and their degraded products give strong absorption peaks in the UV-Vis region and these properties make the reaction to be monitored by a UV-Vis spectrophotometer. There are also various studies on the catalytic degradation of these

dyes as presented with some examples in Section 4.1.1. So it is possible to reach wide information about their degradation process and it allows us to compare our experimental data with previous studies.

Degradation process consists in the electron transfer between the acceptor and donor. On that account, the potential difference between these two species gains an important role for degradation of dyes. Large difference between the redox potentials hampers the electron transfer. Copper nanowires that have a redox potential value between the acceptor and donor's potential values had an important impact to reduce this potential difference in this study.

In an attempt to confirm the catalytic effect of copper nanowires, catalyzed and uncatalyzed degradations of the dyes by $NaBH_4$ were monitored. Figure 4.4.1 shows the UV-Vis absorption spectra of dyes under uncatalyzed degradation reactions. There is a small decrease in the absorbance peak of methylene blue at 663 nm after 60 min which shows the little decrease in the concentration of MB. Absorption of methyl orange at 464 nm hardly changed during the same period. The decrease in Rhodamine B absorption peak at 554 nm appears to be clearer, but the concentration of the dye is still quite high after 60 min. Without using any catalyst, decreases in the absorption intensities of dyes are very low, which is an indication for very low reaction rates. The reaction constants with respect to 0, 1st, and 2nd order reactions for the uncatalyzed degradation processes are shown in Figure 4.4.2.
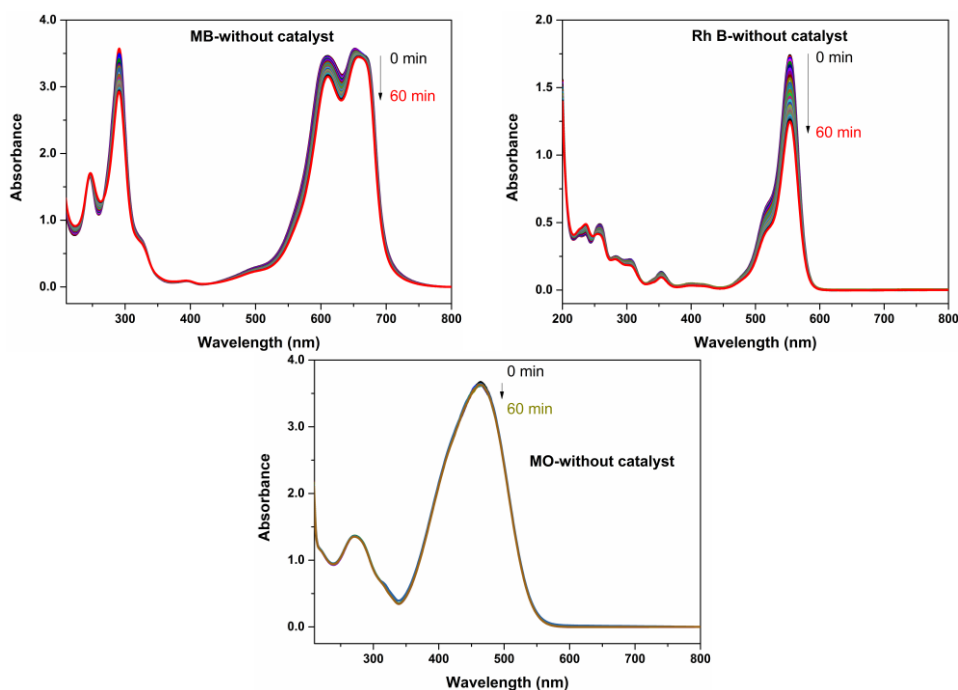
Figure 4.4.1 UV-Vis spectra of uncatalyzed degradation of **a)** Methylene blue **b)** Rhodamine B **c)** Methyl orange.
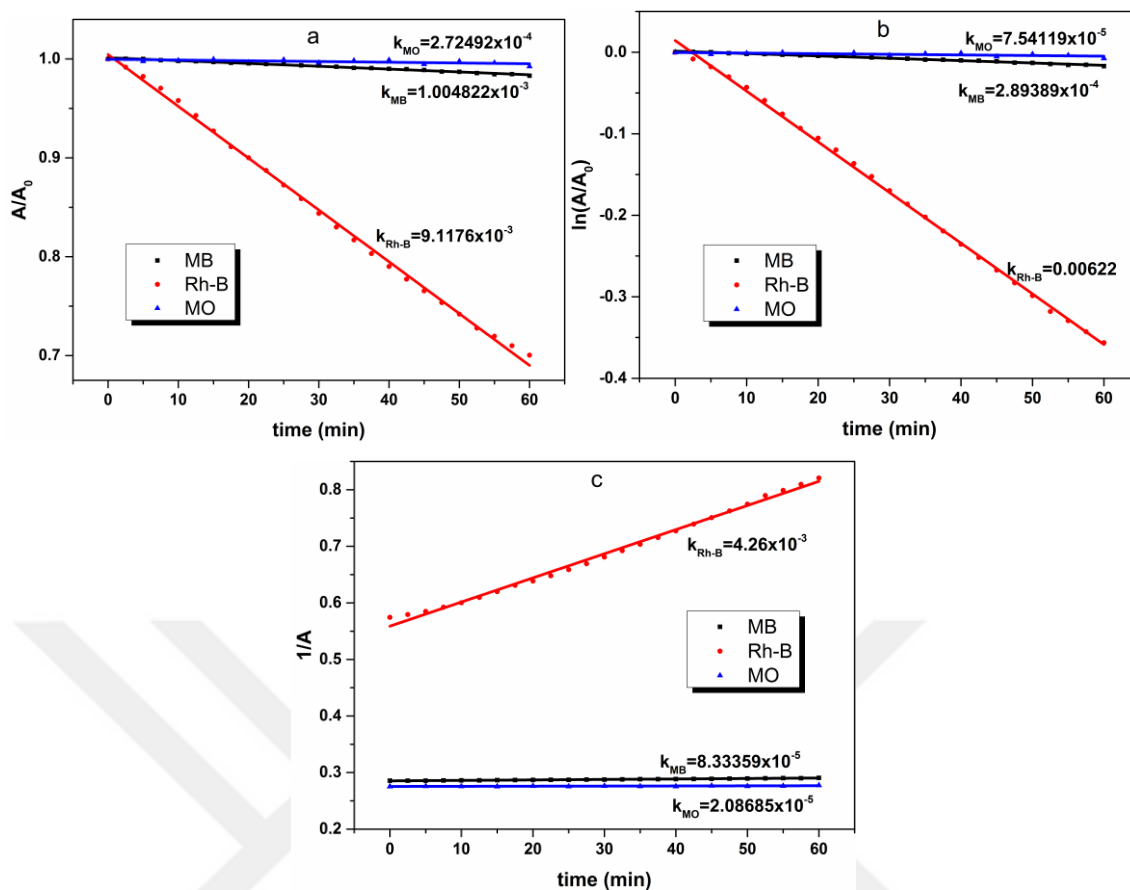
Figure 4.4.2 Uncatalyzed reaction rates for **a)** 0 order **b)** 1st order **c)** 2nd order reactions.

Methylene blue has a maximum absorption peak at λ_{max}=663 nm with a side peak at 612 nm and other peak in the UV region at 291 nm. As a result of reduction by $NaBH_4$, the intensity of these peaks starts decreasing and intensity of a new peak at 246 nm starts increasing by the increase in Leucomethylene blue (LMB) concentration with a red shift. While determining the reaction rates, we considered λ_{max}. As it seen clearly on Figure 4.4.1, reduction of MB into LMB by $NaBH_4$ in the absence of catalyst is not a rapid process and not feasible as a solution to extinguish the harmful effects of MB. Figure 4.4.3 shows the strong effect of copper nanowires on the degradation reaction. Blue color vanished completely in 4 min with catalyst solution contains only 0.2 mg of copper nanowire. On the purpose of understanding how the amount of catalyst affects the reaction rate, degradation process was performed with different amount of catalyst. Even very little amounts of copper nanowire, such as 0.025 mg, speeded the reaction rate up tremendously. Increasing catalyst amount concluded with the increase in reaction rates. Nevertheless, after some catalyst quantity, increment in reaction rate began falling off. As it seen in Figure 4.4.4, the reaction rates for 0.15 mg and 0.2 mg of copper nanowires are almost the same. After this point, increasing the catalyst amount is

not effective. During the reduction of methylene blue, the reverse reaction is also effective, especially on the surface because of the O_2 in air. We observed the color change on the surface of solution back into blue. By gently shaking the solution, blue color disappeared again due to the domination of reduction reaction. To eliminate the effect of reverse reaction, all measurements were performed into capped and completely filled cuvettes. Amount of nanowires is also effective for the stability of the product. When 0.025 mg catalyst was used, the color vanished completely in 10 min but after a few hours, blue color appeared again. This trend wasn't observed higher catalyst quantities.

Maximum absorption peak for Rhodamine B was observed at λ_{max}=554 nm. Uncatalyzed degradation of Rh-B by $NaBH_4$ is more significant compared to the other two dyes as it's clearly seen in Figure 4.4.1 and 4.4.2. After 60 min, approximately a quarter of dye was degraded. This period was reduced to a few minutes by copper nanowire catalyst. While the intensity of absorption peak at 554 nm is decreasing, small peak at 237 nm starts increasing through the degradation process. Reaction rate increases by the increase in amount of CuNW as it's clearly seen in Figure 4.4.5 and Figure 4.4.6. Effect of reversible reaction was also observable for Rh-B as the same with MB. The color started to become pink on the surface after some time so the same precautions were taken during the measurement.

The last organic dye in this study is methyl orange. λ_{max} for this dye was observed at 464 nm wavelength. Without catalyst, $NaBH_4$ didn't have almost any effect for the degradation of the dye alone. The effect of CuNWs for the degradation of MO is clearly seen in Figure 4.4.7. The reaction ended in 4 minutes in the presence of 0.2-0.25 mg CuNW catalyst. While the decrement of absorption peak of methyl orange as a result of consumption of dye, another peak's intensity started to increase between 250-270 nm with a blue shift. Increase in catalyst quantity has also the same effect with MB reduction reaction. Changes in the reaction rates depending on the change in catalyst amount were larger but after 0.25 mg the impact of nanowire quantity increase was not effective as shown in Figure 4.4.8. Reverse reaction of the MO degradation process was not observable opposite to MB case and the color didn't appear again after vanished.

Kinetic graphs of degradation processes for all three dyes show the similar trends. As the Figure 4.4.4, Figure 4.4.6, and Figure 4.4.8 show, degradation reactions occurred in two steps. At the beginning, the reaction rate is low and after some point it speeded up. The slower period was also decreased by the increasing catalyst quantity.
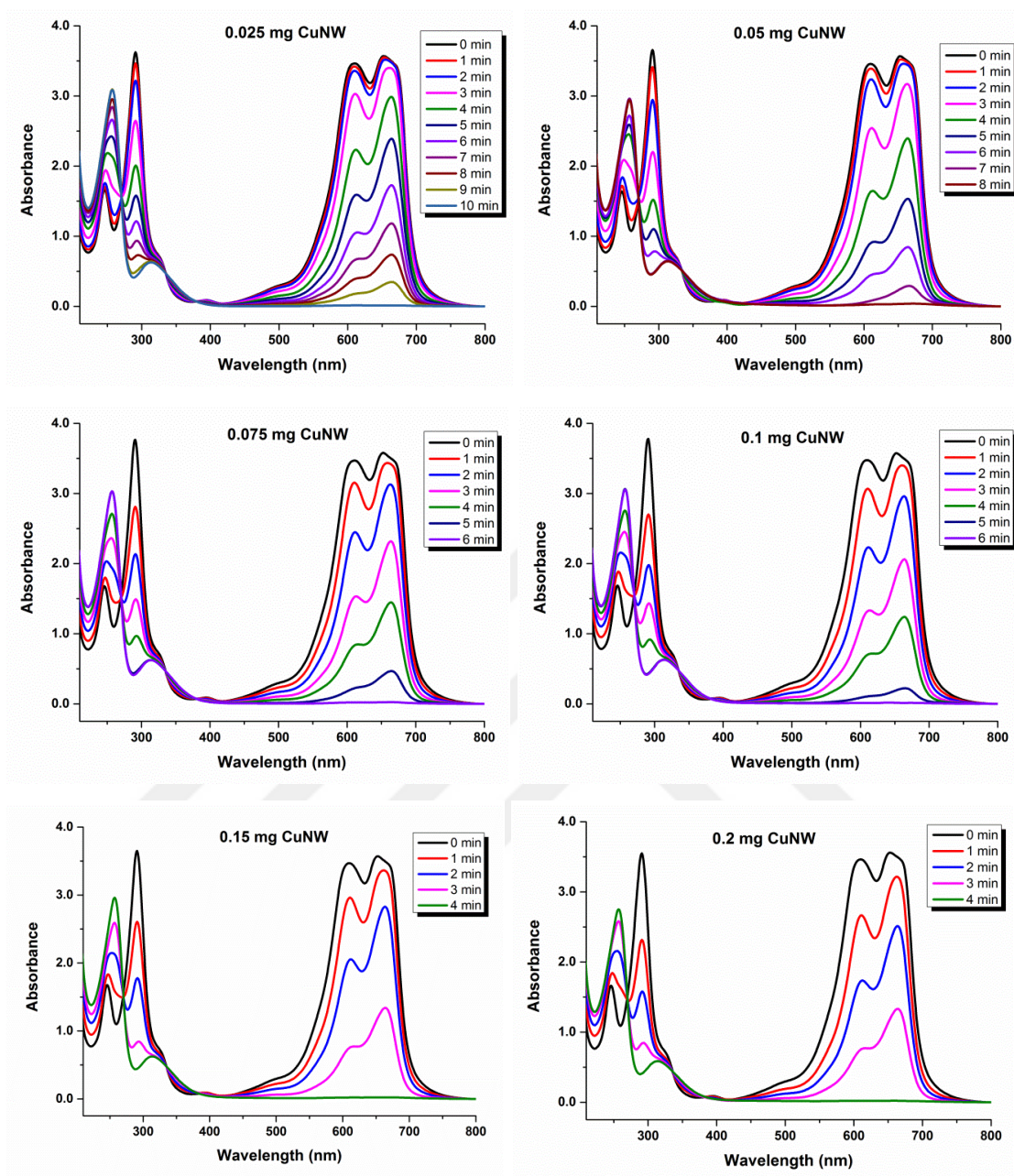
Figure 4.4.3 Comparison graphs of decrease in absorption peaks of MB during catalytic degradation reactions for different catalyst quantities.
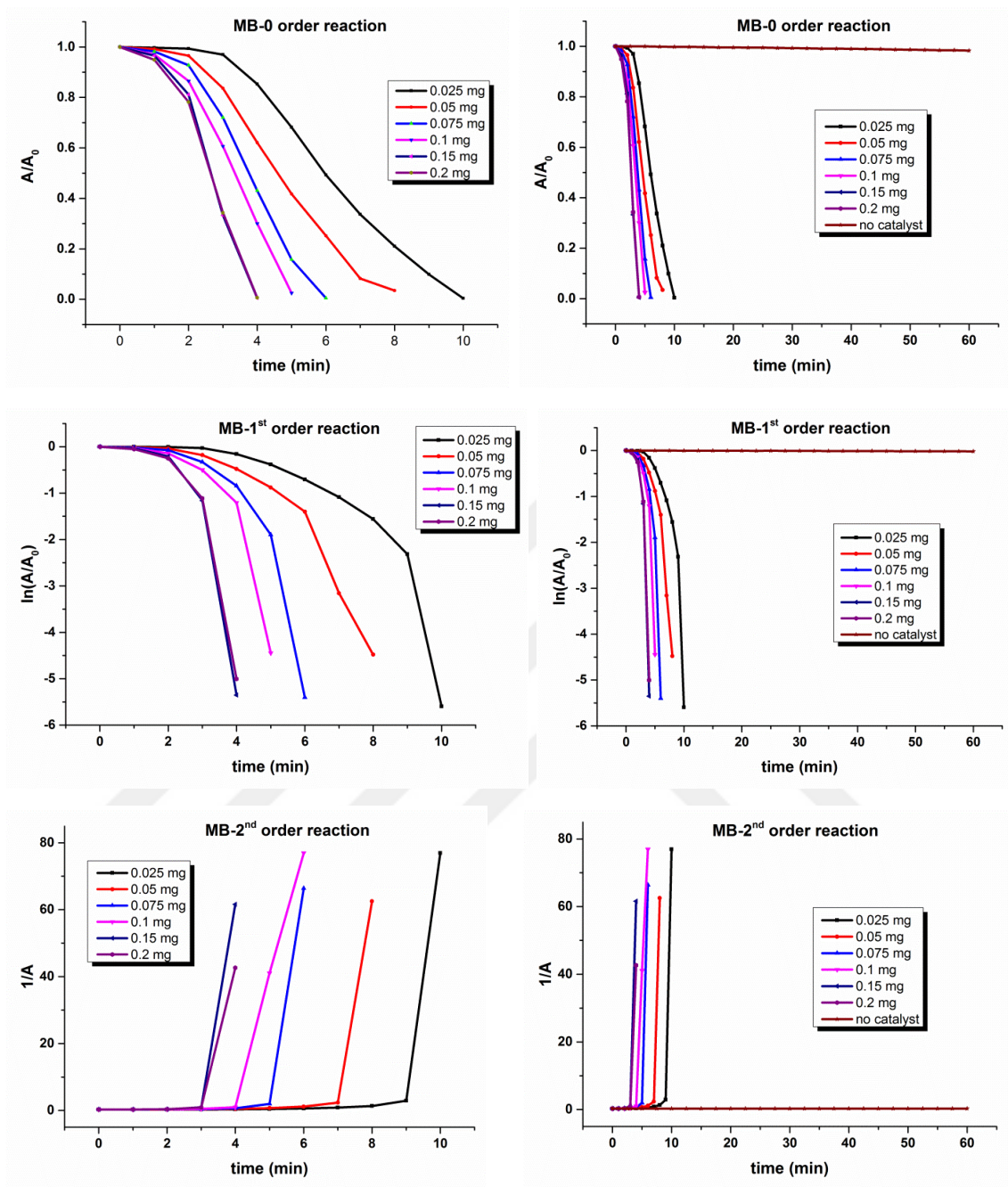
Figure 4.4.4 Kinetic graphs of MB reduction reaction for different order of reactions.
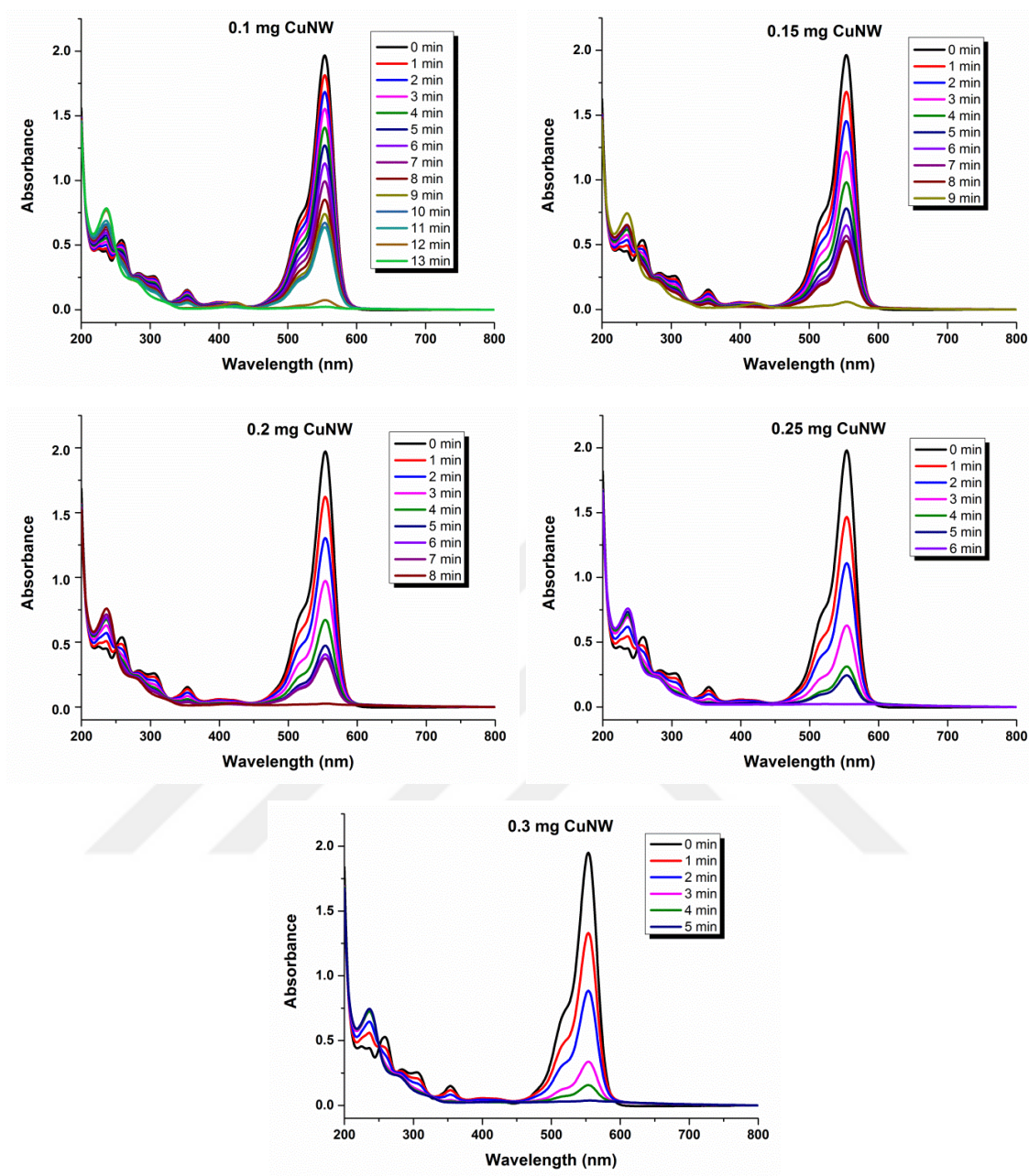
Figure 4.4.5 Comparison graphs of decrease in absorption peaks of Rh-B during catalytic degradation reactions for different catalyst quantities.
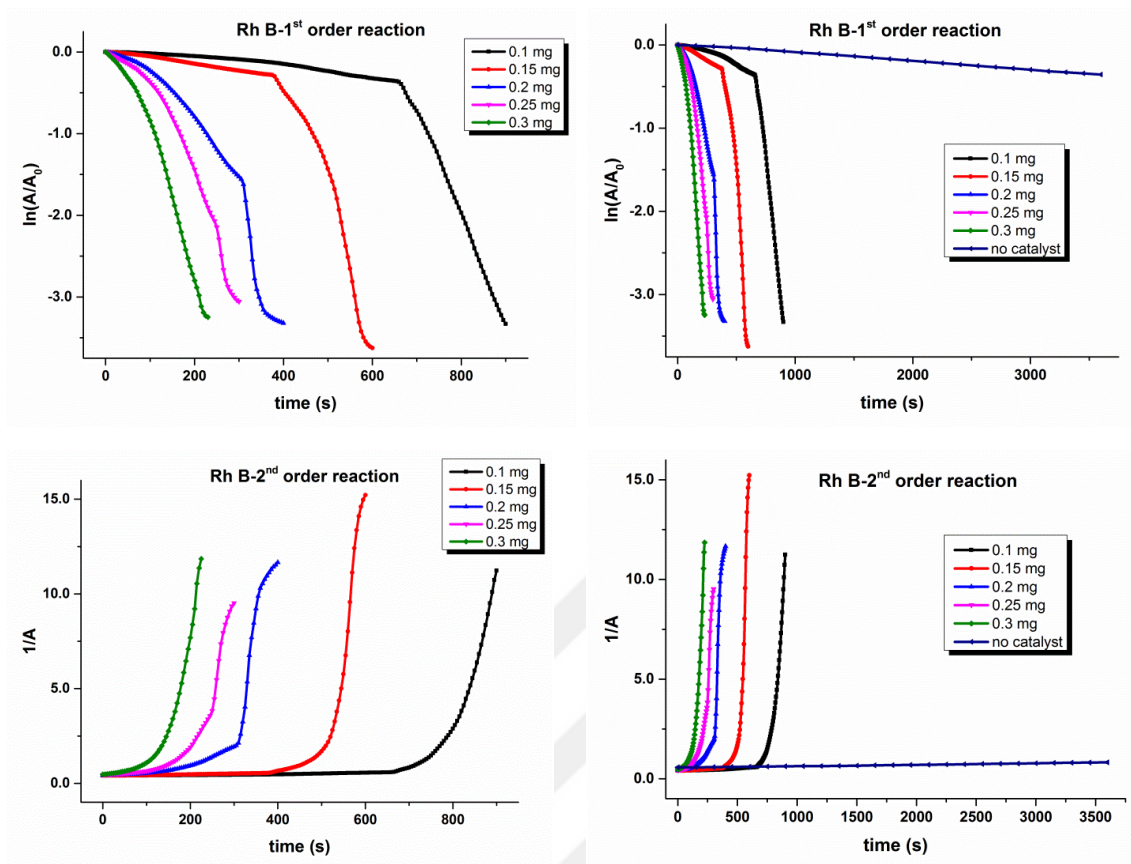
Figure 4.4.6 Kinetic graphs of Rh-B degradation reaction for different order of reactions.
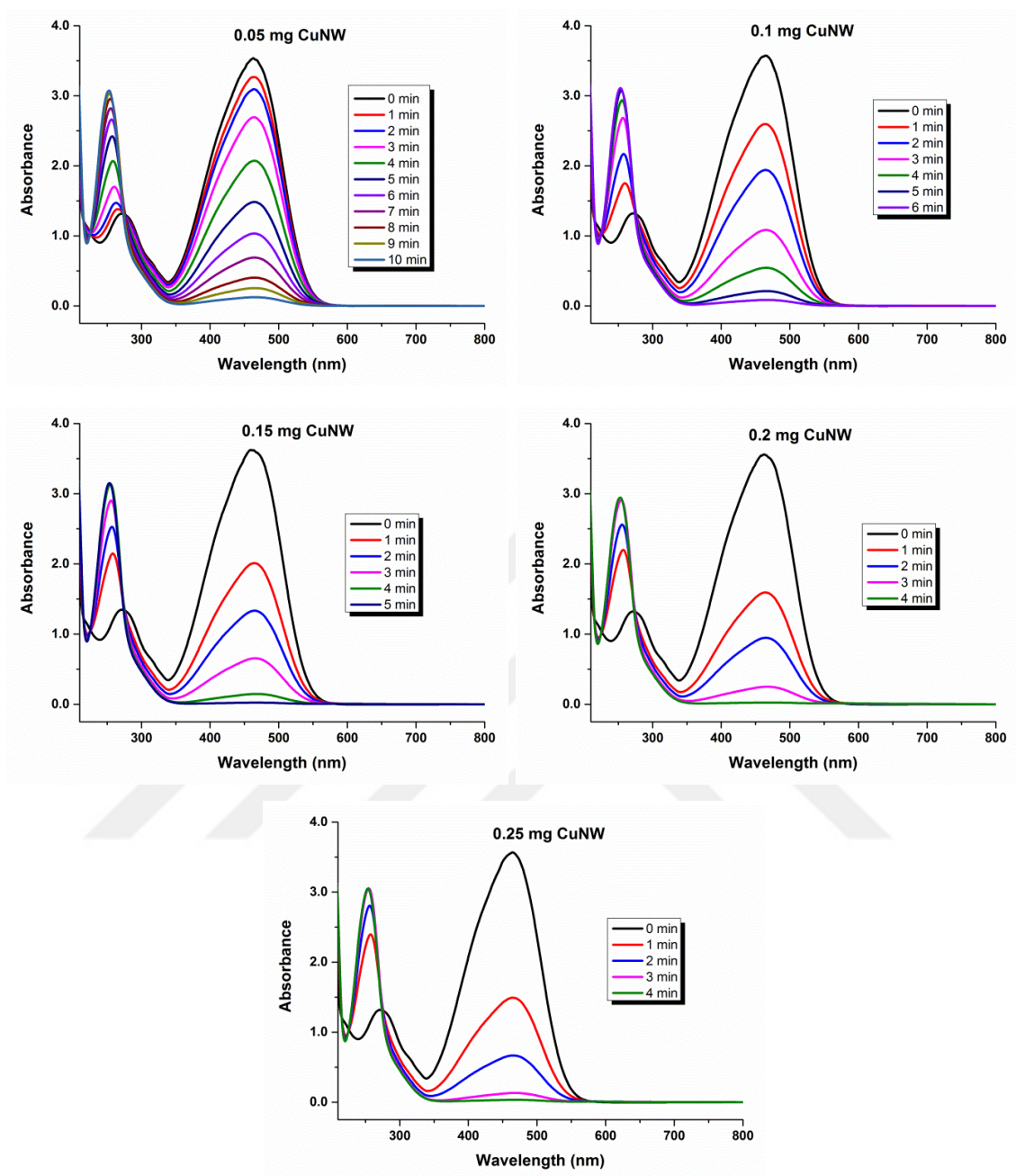
Figure 4.4.7 Comparison graphs of decrease in absorption peaks of MO during catalytic degradation reactions for different catalyst quantities.
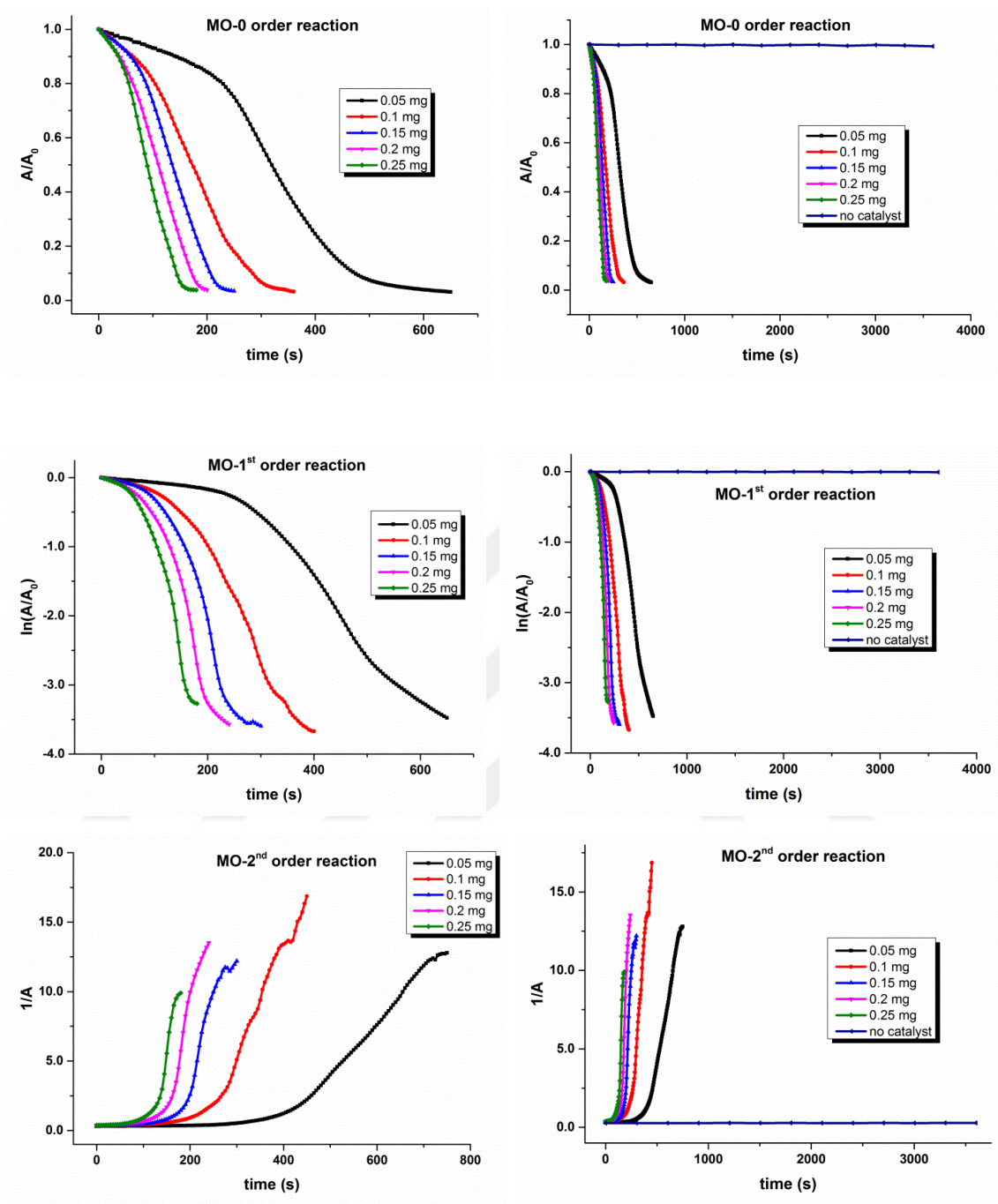
Figure 4.4.8 Kinetic graphs of MO degradation reaction for different order of reactions.

4.5. Conclusion

This chapter reports the catalytic performance of copper nanowires, synthesized via solution based method, on organic dye degradation reactions for methylene blue, rhodamine B, and methyl orange. The reactions were repeated by using different catalyst quantities and the changes in the dye concentrations were monitored by UV-Vis spectrophotometer. The results showed that increasing catalyst amount up to some certain point also increased the rate of reactions. It was also reported that there is a huge difference between the rate of the catalyzed and uncatalyzed reactions for all the dyes. Uncatalyzed reaction rates were found as 7.54119×10^{-5} s^{-1}, 2.89389×10^{-4} s^{-1}, and 6.22×10^{-3} s^{-1} for MO, MB and Rh-B for the 1st order reactions, respectively. It was observed that even very small amounts of CuNW (0.1 mg) catalysts reduced the total degradation period to a few minutes (6 min for MO and MB, 13 min for Rh-B).

Chapter 5

Conclusions and Future Recommendation

5.1. Conclusions

In this study, silver and copper nanowires were synthesized via optimizing some parameters such as temperature, reaction time, and amount of shaping agents. For the synthesis of silver nanowires, effect of molecular weight of PVP molecule and PVP/AgNO$_3$ on nanowire formation was investigated. The best results in terms of aspect ratio for silver nanowires were obtained by using PVP40 molecule at 3.5k PVP/AgNO$_3$ molar ratio. For copper nanowires, while the product of hydrothermal method looks promising for display applications in terms of high aspect ratio and smooth nanowire surface, the nanowires obtained from solution based method were shorter and had rough surface which can be advantageous for catalytic applications. Coating studies with gold, palladium and platinum gave promising results which are important for haze reduction and prevention of nanowires against oxidation.

Catalysis performance of copper nanowires, which were synthesized by solution based method, was investigated for degradation of three organic dyes: methylene blue, rhodamine B and methyl orange in the presence of NaBH$_4$ as reducing agent. The reaction rate for the catalytic degradation reactions increased to a large extent compared to uncatalyzed ones. While small changes in the concentration of dyes could be observed during the uncatalyzed reactions in 1 h, degradations were completed in a few minutes even very small amount of copper nanowires was used.

4.6. Future Recommendation

In this thesis study, it was focused mostly on the synthesis of silver and copper nanowires. For the future work, it can be studied on display applications of these metal nanowire networks by improving the transmittance and sheet resistance. Also, further studies can be performed to improve the coating methods to provide smoother and more homogeneous galvanic exchange. Moreover, catalytic performance of copper nanowires can be investigated for other reactions and effect of coating with noble metals can be studied for catalysis applications. In addition, silver nanowires can also be studied as catalysts.

BIBLIOGRAPHY

[1]   What is nanotechnology?, http://www.nano.gov/nanotech-101/what/definition (01.12.2015)

[2]   Scanning tunneling microscope (STM), http://global.britannica.com/technology/scanning-tunneling-microscope (01.12.2015)

[3]   What's So Special about the Nanoscale, http://www.nano.gov/nanotech-101/special (01.12.2015)

[4]   Properties of Nanomaterials, http://www.nanowerk.com/nanotechnology/introduction/introduction_to_nanotechnology_3.php (01.12.2015)

[5]   K. Bhattacharyya, B. S. Goldschmidt, M. Hannink, S. Alexander, A. Jurkevic, J. A. Viator, "Gold Nanoparticle-Mediated Detection of Circulating Cancer Cells," Clinics in Laboratory Medicine, 32, 89-101 (2012).

[6]   T. Y. Zheng, N. Pierre-Pierre, X. Yan, Q. Huo, A. J. O. Almodovar, F. Valerio, I. Rivera-Ramirez, E. Griffith, D. D. Decker, S. X. Chen, N. Zhu, "Gold Nanoparticle-Enabled Blood Test for Early Stage Cancer Detection and Risk Assessment," ACS Applied Materials & Interfaces, 7, 6819-6827 (2015).

[7]   Y. Cheng, S. L. Wang, R. R. Wang, J. Sun, L. Gao, "Copper nanowire based transparent conductive films with high stability and superior stretchability," Journal of Materials Chemistry C, 2, 5309-5316 (2014).

[8]   P. Lee, J. Lee, H. Lee, J. Yeo, S. Hong, K. H. Nam, D. Lee, S. S. Lee, S. H. Ko, "Highly Stretchable and Highly Conductive Metal Electrode by Very Long Metal Nanowire Percolation Network," Advanced Materials, 24, 3326-3332 (2012).

[9]   D. Q. Zhang, R. R. Wang, M. C. Wen, D. Weng, X. Cui, J. Sun, H. X. Li, Y. F. Lu, "Synthesis of Ultralong Copper Nanowires for High-Performance Transparent Electrodes," Journal of the American Chemical Society, 134, 14283-14286 (2012).

[10]   H. Wu, L. B. Hu, M. W. Rowell, D. S. Kong, J. J. Cha, J. R. McDonough, J. Zhu, Y. A. Yang, M. D. McGehee, Y. Cui, "Electrospun Metal Nanofiber Webs as High-Performance Transparent Electrode," Nano Letters, 10, 4242-4248 (2010).

[11]   S. R. Ye, A. R. Rathmell, Z. F. Chen, I. E. Stewart, B. J. Wiley, "Metal Nanowire Networks: The Next Generation of Transparent Conductors," Advanced Materials, 26, 6670-6687 (2014).

[12]   J. Lee, P. Lee, H. B. Lee, S. Hong, I. Lee, J. Yeo, S. S. Lee, T. S. Kim, D. Lee, S. H. Ko, "Room-Temperature Nanosoldering of a Very Long Metal Nanowire Network by Conducting-Polymer-Assisted Joining for a Flexible Touch-Panel Application," Advanced Functional Materials, 23, 4171-4176 (2013).

[13]   W. W. He, C. H. Ye, "Flexible Transparent Conductive Films on the Basis of Ag Nanowires: Design and Applications: A Review," Journal of Materials Science & Technology, 31, 581-588 (2015).

[14]   D. Langley, G. Giusti, C. Mayousse, C. Celle, D. Bellet, J. P. Simonato, "Flexible transparent conductive materials based on silver nanowire networks: a review," Nanotechnology, 24 (2013).

[15]   Mineral Commodity Summaries 2012, U.S. Geological Survey, (2012).

[16]   Mineral Commodity Summaries 2014, U.S. Geological Survey, (2014).

[17]   D. Angmo, F. C. Krebs, "Flexible ITO-Free Polymer Solar Cells," Journal of Applied Polymer Science, 129, 1-14 (2013).

[18]   PEDOT:PSS, https://en.wikipedia.org/wiki/PEDOT:PSS (01.12.2015)

[19]   T.-H. Han, S.-H. Jeong, Y. Lee, H.-K. Seo, S.-J. Kwon, P. Min-Ho, T.-W. Lee, "Flexible transparent electrodes for organic light-emitting diodes," Journal of Information Display, 16, 71-84 (2015).

[20]   N. Massonnet, A. Carella, A. de Geyer, J. Faure-Vincent, J. P. Simonato, "Metallic behaviour of acid doped highly conductive polymers," Chemical Science, 6, 412-417 (2015).

[21]   N. Kim, S. Kee, S. H. Lee, B. H. Lee, Y. H. Kahng, Y. R. Jo, B. J. Kim, K. Lee, "Highly Conductive PEDOT: PSS Nanofibrils Induced by Solution-Processed Crystallization," Advanced Materials, 26, 2268-2272 (2014).

[22]   Graphene, https://en.wikipedia.org/wiki/Graphene (01.12.2015)

[23]   S. S. Shams, R. Zhang, J. Zhu, "Graphene synthesis: a Review," Materials Science-Poland, 33, 566-578 (2015).

[24]   J. H. Du, S. F. Pei, L. P. Ma, H. M. Cheng, "25th Anniversary Article: Carbon Nanotube- and Graphene- Based Transparent Conductive Films for Optoelectronic Devices," Advanced Materials, 26, 1958-1991 (2014).

[25]   S. S. Yao, Y. Zhu, "Nanomaterial-Enabled Stretchable Conductors: Strategies, Materials and Devices," Advanced Materials, 27, 1480-1511 (2015).

[26]   D. S. Hecht, L. B. Hu, G. Irvin, "Emerging Transparent Electrodes Based on Thin Films of Carbon Nanotubes, Graphene, and Metallic Nanostructures," Advanced Materials, 23, 1482-1513 (2011).

[27]   D. P. Langley, M. Lagrange, G. Giusti, C. Jimenez, Y. Brechet, N. D. Nguyen, D. Bellet, "Metallic nanowire networks: effects of thermal annealing on electrical resistance," Nanoscale, 6, 13535-13543 (2014).

[28]   Table of Electrical Resistivity and Conductivity, http://chemistry.about.com/od/moleculescompounds/a/Table-Of-Electrical-Resistivity-And-Conductivity.htm (01.12.2015)

[29]   A. A. Lewinsky, "Hazardous Materials and Wastewater: Treatment, Removal and Analysis," Nova Publishers, (2007).

[30]   N. Koprivanac, H. Kusic, "Hazardous Organic Pollutants in Colored Wastewaters," Nova Science Publishers, (2009).

[31]   I. Arslan, I. A. Balcioglu, D. W. Bahnemann, "Heterogeneous photocatalytic treatment of simulated dyehouse effluents using novel TiO2-photocatalysts," Applied Catalysis B-Environmental, 26, 193-206 (2000).

[32]   New solution for dye wastewater pollution, http://www.rsc.org/chemistryworld/News/2009/July/08070901.asp (02.12.2015)

[33]   T. Kim, A. Canlier, G. H. Kim, J. Choi, M. Park, S. M. Han, "Electrostatic Spray Deposition of Highly Transparent Silver Nanowire Electrode on Flexible Substrate," ACS Applied Materials & Interfaces, 5, 788-794 (2013).

[34]   T. Tokuno, M. Nogi, M. Karakawa, J. T. Jiu, T. T. Nge, Y. Aso, K. Suganuma, "Fabrication of silver nanowire transparent electrodes at room temperature," Nano Research, 4, 1215-1222 (2011).

[35] T. Kim, A. Canlier, C. Cho, V. Rozyyev, J. Y. Lee, S. M. Han, "Highly Transparent Au-Coated Ag Nanowire Transparent Electrode with Reduction in Haze," ACS Applied Materials & Interfaces, 6, 13527-13534 (2014).

[36] N. M. Abbasi, H. J. Yu, L. Wang, Zain-ul-Abdin, W. A. Amer, M. Akram, H. Khalid, Y. S. Chen, M. Saleem, R. L. Sun, J. Shan, "Preparation of silver nanowires and their application in conducting polymer nanocomposites," Materials Chemistry and Physics, 166, 1-15 (2015).

[37] B. Wiley, Y. G. Sun, B. Mayers, Y. N. Xia, "Shape-controlled synthesis of metal nanostructures: The case of silver," Chemistry-A European Journal, 11, 454-463 (2005).

[38] Y. G. Sun, Y. D. Yin, B. T. Mayers, T. Herricks, Y. N. Xia, "Uniform silver nanowires synthesis by reducing AgNO3 with ethylene glycol in the presence of seeds and poly(vinyl pyrrolidone)," Chemistry of Materials, 14, 4736-4745 (2002).

[39] S. Hong, H. Lee, J. Lee, J. Kwon, S. Han, Y. D. Suh, H. Cho, J. Shin, J. Yeo, S. H. Ko, "Highly Stretchable and Transparent Metal Nanowire Heater for Wearable Electronics Applications," Advanced Materials, 27, 4744-4751 (2015).

[40] S. Coskun, B. Aksoy, H. E. Unalan, "Polyol Synthesis of Silver Nanowires: An Extensive Parametric Study," Crystal Growth & Design, 11, 4963-4969 (2011).

[41] B. Wiley, T. Herricks, Y. G. Sun, Y. N. Xia, "Polyol synthesis of silver nanoparticles: Use of chloride and oxygen to promote the formation of single-crystal, truncated cubes and tetrahedrons," Nano Letters, 4, 1733-1739 (2004).

[42] S. E. Skrabalak, B. J. Wiley, M. Kim, E. V. Formo, Y. N. Xia, "On the polyol synthesis of silver nanostructures: Glycolaldehyde as a reducing agent," Nano Letters, 8, 2077-2081 (2008).

[43] Y. D. Yin, Y. Lu, Y. G. Sun, Y. N. Xia, "Silver nanowires can be directly coated with amorphous silica to generate well-controlled coaxial nanocables of silver/silica," Nano Letters, 2, 427-430 (2002).

[44] Y. G. Sun, "Conversion of Ag Nanowires to AgCl Nanowires Decorated with Au Nanoparticles and Their Photocatalytic Activity," Journal of Physical Chemistry C, 114, 2127-2133 (2010).

[45] Y. G. Sun, "Silver nanowires - unique templates for functional nanostructures," Nanoscale, 2, 1626-1642 (2010).

[46] Y. Y. Jiang, Y. Z. Lu, D. X. Han, Q. X. Zhang, L. Niu, "Hollow Ag@Pd core-shell nanotubes as highly active catalysts for the electro-oxidation of formic acid," Nanotechnology, 23 (2012).

[47] A. Canlier, U. V. Ucak, H. Usta, C. Cho, J. Y. Lee, U. Sen, M. Citir, "Development of highly transparent Pd-coated Ag nanowire electrode for display and catalysis applications," Applied Surface Science, 350, 79-86 (2015).

[48] H. G. Im, S. H. Jung, J. Jin, D. Lee, J. Lee, D. Lee, J. Y. Lee, I. D. Kim, B. S. Bae, "Flexible Transparent Conducting Hybrid Film Using a Surface-Embedded Copper Nanowire Network: A Highly Oxidation-Resistant Copper Nanowire Electrode for Flexible Optoelectronics," ACS Nano, 8, 10973-10979 (2014).

[49] Z. Yin, C. Lee, S. Cho, J. Yoo, Y. Piao, Y. S. Kim, "Facile Synthesis of Oxidation-Resistant Copper Nanowires toward Solution-Processable, Flexible, Foldable, and Free-Standing Electrodes," Small, 10, 5047-5052 (2014).

[50] S. Zhong, T. Koch, M. Wang, T. Scherer, S. Walheim, H. Hahn, T. Schimmel, "Nanoscale Twinned Copper Nanowire Formation by Direct Electrodeposition," Small, 5, 2265-2270 (2009).

[51] Z. W. Liu, Y. Bando, "A novel method for preparing copper nanorods and nanowires," Advanced Materials, 15, 303-305 (2003).

[52] J. C. Zhou, C. M. Soto, M. S. Chen, M. A. Bruckman, M. H. Moore, E. Barry, B. R. Ratna, P. E. Pehrsson, B. R. Spies, T. S. Confer, "Biotemplating rod-like viruses for the synthesis of copper nanorods and nanowires," Journal of Nanobiotechnology, 10, 18-29 (2012).

[53] Y. Shi, H. Li, L. Q. Chen, X. J. Huang, "Obtaining ultra-long copper nanowires via a hydrothermal process," Science and Technology of Advanced Materials, 6, 761-765 (2005).

[54] Y. Chang, M. L. Lye, H. C. Zeng, "Large-scale synthesis of high-quality ultralong copper nanowires," Langmuir, 21, 3746-3748 (2005).

[55] Y. B. Ren, S. C. Zhang, R. X. Lin, X. Wei, "Electro-catalytic performance of Pd decorated Cu nanowires catalyst for the methanol oxidation," International Journal of Hydrogen Energy, 40, 2621-2630 (2015).

[56] J. Zheng, D. A. Cullen, R. V. Forest, J. A. Wittkopft, Z. B. Zhuang, W. C. Sheng, J. G. G. Chen, Y. S. Yan, "Platinum-Ruthenium Nanotubes and Platinum-Ruthenium Coated Copper Nanowires As Efficient Catalysts for Electro-Oxidation of Methanol," ACS Catalysis, 5, 1468-1474 (2015).

[57] Z. F. Chen, S. R. Ye, A. R. Wilson, Y. C. Ha, B. J. Wiley, "Optically transparent hydrogen evolution catalysts made from networks of copper-platinum core-shell nanowires," Energy & Environmental Science, 7, 1461-1467 (2014).

[58] S. M. Alia, K. Jensen, C. Contreras, F. Garzon, B. Pivovar, Y. S. Yan, "Platinum Coated Copper Nanowires and Platinum Nanotubes as Oxygen Reduction Electrocatalysts," ACS Catalysis, 3, 358-362 (2013).

[59] A. R. Rathmell, S. M. Bergin, Y. L. Hua, Z. Y. Li, B. J. Wiley, "The Growth Mechanism of Copper Nanowires and Their Properties in Flexible, Transparent Conducting Films," Advanced Materials, 22, 3558-3563 (2010).

[60] J. Tiana, Y. Leng, H. Cuia, H. Liub, "Hydrogenated TiO^2 nanobelts as highly efficient photocatalyticorganic dye degradation and hydrogen evolution photocatalyst," Journal of Hazardous Materials, 299, 165–173 (2015).

[61] A. Mondal, B. Adhikary, D. Mukherjee, "Room-temperature synthesis of air stable cobalt nanoparticles and their use as catalyst for methyl orange dye degradation," Colloids and Surfaces a-Physicochemical and Engineering Aspects, 482, 248-257 (2015).

[62] A. M. a. D. M. Arijit Mondal, "Room-temperature synthesis of cobalt nanoparticles and their use as catalysts for Methylene Blue and Rhodamine-B dye degradation," Advances in Nano Research, 3, 67-79 (2015).

[63] P. Ncube, N. Bingwa, H. Baloyi, R. Meijboom, "Catalytic activity of palladium and gold dendrimer-encapsulated nanoparticles for methylene blue reduction: A kinetic analysis," Applied Catalysis A: General, 495, 63-71 (2015).

[64] N. Gupta, H. P. Singh, R. K. Sharma, "Metal nanoparticles with high catalytic activity in degradation of methyl orange: An electron relay effect," Journal of Molecular Catalysis A: Chemical, 335, 248-252 (2011).

[65] K. Sharma, G. Singh, M. Kumar, V. Bhalla, "Silver nanoparticles: facile synthesis and their catalytic application for the degradation of dyes," RSC Advances, 5, 25781–25788 (2015).

[66] V. K. Vidhu, D. Philip, "Catalytic degradation of organic dyes using biosynthesized silver nanoparticles," Micron, 56, 54-62 (2014).

[67] H. Feng, Y. Li, S. Lin, E. V. V. d. Eycken, G. Song, "Nano Cu-catalyzed efficient and selective reduction of nitroarenes under combined microwave and ultrasound irradiation," Sustainable Chemical Processes, 2, 14 (2014).

[68] R. A. Soomro, A. Nafady, Sirajuddin, S. T. H. Sherazi, N. H. Kalwar, M. R. Shah, K. R. Hallam, "Catalytic Reductive Degradation of Methyl Orange Using Air Resilient Copper Nanostructures," Journal of Nanomaterials, 1-13 (2015).

[69] Y. Zhang, P. Zhu, L. Chen, G. Li, F. Zhou, D. Lu, R. Sun, F. Zhou, C.-p. Wong, "Hierarchical architectures of monodisperse porous Cu microspheres: synthesis, growth mechanism, high-efficiency and recyclable catalytic performance," Journal of Materials Chemistry A, 2, 11966 (2014).

[70] L. Xia, H. Zhao, G. Liu, X. Hu, Y. Liu, J. Li, D. Yang, X. Wang, "Degradation of dyes using hollow copper microspheres as catalyst," Colloids and Surfaces A: Physicochemical and Engineering Aspects, 384, 358-362 (2011).

[71] S. Bala, S. Bhattacharya, A. Goswami, A. Adhikary, S. Konar, R. Mondal, "Designing Functional Metal-Organic Frameworks by Imparting a Hexanuclear Copper-Based Secondary Building Unit Specific Properties: Structural Correlation With Magnetic and Photocatalytic Activity," Crystal Growth & Design, 14, 6391-6398 (2014).

[72] H. Hu, M. W. Shao, W. Zhang, L. Lu, H. Wang, S. Wang, "Synthesis of layer-deposited silicon nanowires, modification with Pd nanoparticles, and their excellent catalytic activity and stability in the reduction of methylene blue," Journal of Physical Chemistry C, 111, 3467-3470 (2007).

[73] C. Ray, S. Dutta, S. Sarkar, R. Sahoo, A. Roy, T. Pal, "A facile synthesis of 1D nano structured selenium and Au decorated nano selenium: catalysts for the clock reaction," RSC Advances, 3, 24313 (2013).

[74] C. Sachse, N. Weiss, N. Gaponik, L. Muller-Meskamp, A. Eychmuller, K. Leo, "ITO-Free, Small-Molecule Organic Solar Cells on Spray-Coated Copper-Nanowire-Based Transparent Electrodes," Advanced Energy Materials, 4 (2014).

[75] S. L. Wang, Y. Cheng, R. R. Wang, J. Sun, L. Gao, "Highly Thermal Conductive Copper Nanowire Composites with Ultralow Loading: Toward Applications as Thermal Interface Materials," ACS Applied Materials & Interfaces, 6, 6481-6486 (2014).

[76] J. A. Wittkopf, J. Zheng, Y. S. Yan, "High-Performance Dealloyed PtCu/CuNW Oxygen Reduction Reaction Catalyst for Proton Exchange Membrane Fuel Cells," ACS Catalysis, 4, 3145-3151 (2014).